PSEUDO-COMPONENT VISCOELASTIC MODELING OF SOFT TISSUES

By

UPASANA MANIMEGALAI SRIDHAR

Bachelor of Technology in Chemical Engineering

Sri Sivasubramaniya Nadar College of Engineering

Anna University

Chennai, Tamil Nadu, India

2009

Submitted to the Faculty of the
Graduate College of the
Oklahoma State University
in partial fulfillment of
the requirements for
the Degree of
MASTER OF SCIENCE
December, 2010

PSEUDO-COMPONENT VISCOELASTIC

MODELING OF SOFT TISSUES

Thesis Approved:

Dr. R Russell Rhinehart

Thesis Adviser

Dr. Arland H Johannes

Dr. Sundar V Madihally

Dr. Mark E. Payton

Dean of the Graduate College

ACKNOWLEDGMENTS

First and foremost I would like to express my deepest gratitude to my advisor Dr. R. Russell Rhinehart. I am grateful for his relentless guidance, insurmountable patience and encouragement. Without his inspiring guidance this thesis would have never been possible. I have gained a lot by interacting with him and it has been an honor being part of Dr. R. Russell Rhinehart's research team. I also feel it is my bounden duty to thank him for providing me with financial assistance during my period of stay at OSU.

I would like to express my heartiest thanks to my committee members, Dr. Sundar. V. Madihally and Dr. Arland. H. Johannes for their interest in my research. I would like to specially thank Dr. Sundar for helping me complete my research by providing me with data and ideas.

A special thanks to Kornkorn Makornkaewkeyoon, Rahul Mirani and Swapnika Ratakonda for sharing their data with me.

With a deep sense of gratitude I would like to thank my brother and friend Anand Govindarajan who was a constant source of encouragement throughout my period of study. I also thank him for his constant support, help and interest in my research. Successful entry as a Master's student would have been impossible without him. I also thank my friends Suresh Kumar, Venkatesh, Krishna, Shubha and Preethi for their constant help, encouragement and interest in my well being. I am very much indebted beyond the ambit of terms for the constant help, guidance and valuable comments provided by my lab mate and friend Anirudh Patrachari. I would be failing in my duty if I don't thank my friend and lab mate Solomon Gebreyohannes for his interest in my research.

I thank my roommates Gargeyi, Pallavi, Anagha and Kavitha; all my friends Harita, Preeti, Raunak, Revathy, Kumar, Krishnan, Sharmila, Sravanthi and Anil, and the Department of Chemical Engineering for their continuous inspiration and timely succor in providing continuous support throughout my stay at OSU.

Heartiest thanks to my friend Sharath Kumar for his relentless support in helping me with many things in India during my period of study at OSU. I also thank him for being an unfailing source of help.

Finally, I thank my brother Swaparjith, father Sridhar, mother Kalavathi, my cousin and friend Rajes for their love and encouragement. I also thank them for being my moving spirit and helping me in all my pursuits.

.

I dedicate this thesis

to my brother and friend

Anand Govindarajan

TABLE OF CONTENTS

LIST OF TABLES

Table Page

LIST OF FIGURES

Figure Page

CHAPTER 1

INTRODUCTION

1.1 Biomedical Engineering [1]*

Understanding the response of human tissues to externally imposed stress and strain is critical to improving the quality of life and health care. Examples include: i) Improvements in automotive safety devices such as air bags and seat belts depend on better knowledge of how human parts, and the whole body, respond to the stresses of impact, ii) Development of biomedical imaging techniques that observe *in vivo* tissue and organ responses to stresses and strains could be used to assess whether a tissue is functioning correctly or needs urgent care when the stress-strain patterns were characterized, iii) Development of synthetic prosthetic devices and *in vitro* regenerated tissues require scaffolds that duplicate mechanical properties of native tissues, iv) Development of simulators that train next-generation physicians and development of robotic procedures both depend on models of the tissue stress-strain response.

* Reference citations in headings indicate that substantial portions are duplicated or modified from that reference

1.2 Viscoelastic Models [1]

For the many reasons stated above, significant efforts have been focused towards developing models of stress-strain behavior of biological materials. The efforts reveal that the biological tissues show a more complex mechanical behavior than polymers, plastics, and metal films [2-14] and they are also found to be anisotropic [15-18]. Hence, conventional models cannot be used to represent these materials.

Many viscoelastic models have been proposed to describe the behavior of biological materials. Fung [3] introduced the Quasi Linear Viscoelastic (QLV) model which was the most utilized phenomenological model of viscoelastic behavior. It was subsequently modified in order to comply with other requirements by many others [9, 19-24]. Unfortunately, the QLV models were incapable in modeling nonstationary, nonlinear, and confounding aspects of the viscoelastic deformation and relaxation mechanisms of biological tissue structures [4-9]. Alternatively, the classical spring-dashpot constitutive models have also been modified to include nonlinear elastic behavior. But, they did not perform in a way that reflected either the mechanistic understanding or phenomenological fidelity of the biological materials such as reduction in the cross sectional area of the material when stretched, etc, [25-29]. In this project, a simple, flexible, useful, mechanistic, and accurate model that is comprised of several pseudo-components which reflect distinct mechanisms of the biological tissue was developed. The model will be tested on a variety of synthetic polymeric tissue substitutes and naturally formed matrix rich in collagen fibers. These choices are designed to express a range of viscoelastic properties.

1.3 Objective [1]

There are four aims in the modeling vision of this work:

First: Tissue stress relaxes in time under constant strain. Also, tissue shape progressively deforms under constant load and tissues gradually return toward original structure when external stress or strain is relieved. Because of all the above stated reasons time-dependent (viscoelastic) models are required. The time-dependent behavior also depends on the stress-strain history. Further, since tissues are comprised of several participating structures (cells, matrix, fibrils, etc.), each having an individual mechanism; a multi-component, viscoelastic model is required. Also, since tissue properties are not constant; nonlinear, multi-component, viscoelastic models are required. Finally, since many tissue components do not relax fully to the original internal structure, the commonly employed dashpot element (which lets the spring return to zero stress) is inappropriate. New constitutive relations are required for the nonlinear, multi-component, viscoelastic models. This work has devised appropriate nonlinear viscoelastic relations and a pseudo-component approach for modeling the viscoelastic behavior of complex tissue structures.

Second: Optimizing viscoelastic model parameter values to best match the model with the experimental stress-strain-time data is difficult because of the presence of multiple local optima. This makes the approaches to the minima often exasperatingly slow (even with classic best practice nonlinear optimizers such as Rhinehart modified Levenberg Marquardt optimization technique). Further, optimization must include constraints on the parameter values, suggesting that direct search methods may be more appropriate than

gradient based methods. Accordingly, techniques such as best-of-N starts [30] should be investigated for determining the probable global optimum subject to multiple constraints. This work will explore the applicability of emerging optimization techniques for obtaining model parameters that better fit the experimental data.

A new optimization technique called Leapfrogging is also explored [31]. This technique starts with a set of players (trial solutions) located randomly in the decision variable (DV) space. During every iteration, this technique relocates the position of the players by reflecting the player with the worst objective function (OF) value across the player with the best OF value. Test cases on this technique revealed that this technique gave better optimized values when compared to other techniques with lower function evaluations.

Third: Macro-scale models can be used to reject or accept proposed constitutive relations of the micro-scale. However, classic regression techniques that accept a "best" model are related to minimizing the overall sum-of-squared-deviations relative to the number of model parameters. These techniques do not indicate whether the constitutive relations within a model are right or wrong. A better model (in a least squares sense) does not mean either that a mechanism has been identified or that a parameter value has interpretable meaning. This work will apply qualitative techniques to judge the utility and appropriateness of models.

Fourth: Viscoelastic results reported in literature depend on regression optimization parameters and choices, and on how assumptions are incorporated in the models. As a

result, the literature lacks consistent analysis. This work will develop pseudo-component models and a nonlinear optimizer in Visual Basic for Applications, which is included in Microsoft Excel®, and the code will be available to the community, providing convenient access, commonality of communication, and an open system for others to add pseudo-component constitutive relations.

However, within the scope of this thesis the pseudo-component element models optimization algorithm had already been developed. This work

1) Explored appropriate model architecture of pseudo-component elements.
2) Evaluated optimizer performance.
3) Explored translation of the models from sequential strain-and-hold stages to predict cyclic loading behavior.
4) Explored model fitting to multiple samples simultaneously.
5) Explored model extrapolation to the next strain-and-hold stage.

CHAPTER 2

BACKGROUND

Failure of organs, loss of tissue due to trauma and disease are some of the most serious problems in health care of human beings [32]. On an average, in the USA, each year at least 8 million surgical procedures are conducted to address failure of organs and tissue care, whose cost exceeds $400 billion every year [33]. Organ replacement has been the technique that was used in most of the places to treat organ loss [34]. The Ohio Solid Organ Transplantation Consortium (OSOTC) established in 1984 by the Ohio Department of Health conducted almost 5,000 transplant candidate reviews, out of which 2,300 patients acquired nonrenal organ transplantation over a span of 15 years [35]. According to the statistics from United Network of Organ Sharing (UNOS) the number of people needing organ transplantation is almost twice the number of donors available [36]. Reconstructive surgery is also being performed of late for correcting disorders like hemi-facial palsy [37]. Chronic discomfort is a long-term problem that results due to surgical reconstruction [38]. However, the techniques mentioned above are not the best solution for treating organ loss or tissue replacement. Organ transplantation remains a challenge because of the infection caused after organ transplantation [39] and also due to donor shortage. In order to provide alternative treatment solutions the field of Biomedical Engineering was developed.

2.1 Tissue and Biomedical Engineering

Tissue Engineering is developed as an interdisciplinary field which combines the knowledge of life sciences and engineering towards aiding organ or tissue repair or replacement [33]. It has been found that one probable solution for tissue regeneration can be the usage of biodegradable scaffolds [40]. Scaffolds generated after removing the cellular components from tissues [41] or from synthetic or natural polymers [42] have been used for the purpose of tissue regeneration. Biocompatibility and biodegradability are two essential qualities that the tissue scaffold should possess so that long-term complications are not encountered [33, 43] and also they should aid in favorable interaction between cells [32]. Many materials were investigated for this purpose and it was found that polymers had a variety of properties that were adjustable and hence the usage of polymers for scaffold formation was further explored [32].

2.2 Natural Matrix

All naturally occurring matrices and their chemical derivatives belong to this group. Their usage in tissue engineering is because of their availability, biocompatibility and biodegradability. Many natural polymers like chitosan, gelatin and glycosaminoglycans are used in tissue engineering applications [32].

Chitosan tends to form a porous structure by the process of lyophilizing and freezing chitosan solution [32]. It has the advantage of helping in anti-microbial activity [44]. Chitosan has the disadvantage of possessing very low break strain [45] and also becomes very rigid and brittle in comparison with soft tissues [32]. The anti-bacterial

functionality of chitosan makes it required in the field of tissue engineering. In order to enhance the polymer properties other polymers are blended with chitosan to make scaffolds [46]. Scaffolds made from both gelatin and chitosan were examined for their usage in tissue regeneration [47], bone tissue and cartilage tissue regeneration [48]. The synthetic analogue of gycosaminoglycans is dextran sulphate. Dextran sulphate is derived from dextran [32] . The advantage of dextran sulphate is that it can be used as an anticoagulant, replacement for blood plasma [49] and also for hydrogel formation which is very widely needed in tissue engineering [50-51].

The advantage of naturally formed matrices is that they facilitate cell attachment and differentiation and the disadvantage is that they have large batch production difficulties [52]. Also scaffolds formed by using natural polymers turn out to be mechanically weak in delivering the body tissue stresses [53]. The disadvantages of natural polymers led to the exploration of synthetic matrixes as scaffolds [5, 45, 54-56].

Small Intestine Sub mucosa (SIS) is a natural scaffold that is used widely in tissue engineering applications. It is isolated from bovine intestines after the muscular, serosal and mucosal layers are removed from the intestine. SIS finds its application in bladder augmentation [57], hernia repair [58-59] and wound healing [60]. However, the usage prediction of SIS in the field of tissue engineering cannot be with a high level of confidence because of the production of large sets of very similar samples [40]. The natural polymer gelatin which is derived from collagen is explored widely for use in tissue engineering because of its extensive nature to form gels when in combination with water [47, 55, 61-63]

2.3 Synthetic Matrix

Synthetic matrices are chemically synthesized from monomers possessing various functional groups [32]. Their usage in the field of tisssue engineering has been examined for more than 10 years [64-65]. Synthetic matrices were formed from biodegradable polymers such as PolyLactic Acid (PLA), polycaprolactone (PCL), PolyGlycolic Acid (PGA), PolyLactic-co-Glycolic Acid (PLGA) [66-67]. The advantage of using a synthetic matrix is that it makes production in large scale reliable and practical as it provides good control over its own properties. The disadvantage of synthetic matrices is the difficulty in matching its mechanical properties to human tissues. This has initiated the search for other techniques in order to develop novel biomaterials. One technique to solve this problem was to blend natural and synthetic polymers which will result in scaffolds having a wide range of properties and scaffolds having mechanical properties that can be adjusted [56, 68-69]. The various techniques used to blend the polymers were grafting [70], freezing and freeze drying [71]. Pok *et al* [72] explored the scaffold formed by self assembled PCL for tissue engineering applications.

PCL and PLGA were of specific interest to the current study. Synthetic PCL [73-74] created lots of interests in the biomedical field [75], as it proved to be compatible with both soft and hard tissues [76]. Low melting point, good mechanical properties, ability to adapt its properties to the tissue requirement by adjusting its molecular weight created more interests and attracted it to the field of tissue engineering [77]. PCL matrices formed after dissolving them in chloroform showed that they could be elongated up to 1000% before they break [78]. The disadvantage of PCL is its poor wetting characteristics because of which uniform distribution of cell adhesion molecules and

proteins does not happen [79]. Also, because of poor cell adhesion their regulation in cellular activity is poor [80]. Hence, PCL is widely used as a tissue engineering template[79]. In order to improve these properties, grafting PCL with RGD peptides was attempted [81-82]. However the growth factor activity of the substrate along with cell migration of the substrate and proliferation of the substrate to regulate the biological response had to be addressed [32].

PLGA is a copolymer that is formed from two monomers, lactic acid and glycolic acid both of which can deal with the human body easily. PLGA can easily be decomposed into its two monomers on hydrolysis [40]. The individual composition of the monomers in PLGA can be varied [40]. Out of all the compositions, PLGA formed using 50% glycolic acid and 50% lactic acid exhibits fastest degradation [71].

2.4 Formation of scaffolds [40]

There is no single ideal fabrication method to form scaffolds. Each method has its own advantages and disadvantages. The fabrication technique for a scaffold extensively depends on the native tissue that needs to be regenerated. The fabrication techniques used for formation of scaffolds are 3D printing [83-84], freeze drying [85], gas foaming [86] and solvent casting and particulate leaching (SCPL) [87-88].

The major disadvantage with SCPL technique is that it uses organic solvents which need to be completely removed before the cells are seeded onto the surface of the scaffold in order to avoid damage of the cells [89]. The usage of organic solvents was done away with gas foaming technique. This technique uses compression molding to

generate a disc shaped structure that was made from a polymer of specific interest. The discs that were formed were then exposed to carbondioxide at high pressure to form sponge like structures [89].

3D printing uses 3D design developed using CAD software [83-84]. The 3D design is then used to form scaffolds by using ink jet printing of the desired polymer melt. The major advantage of 3D printing is that the pore size and the porosity of the scaffold can be adjusted and controlled as per the user's choice [89].

Freeze-drying is the most common and fastest method used to form porous structures from the desired polymers [40].

2.5 Mechanical Analysis

It is important in the field of tissue engineering to focus studies on properties of scaffolds like measuring porosity and degradation characteristics of the scaffold and the materials used to make scaffolds. Studies on the chemical properties of scaffolds show that scaffolds possess properties like cell-binding sites which help in cell attachment. Physical properties of scaffolds like void fraction and pore size stand as cues to help in cell colonization [90]. Studies also show that the surface features of scaffolds like grooves, roughness and edges also have an impact on cell behavior [91-92]. Advances in the area of scaffolds also showed that cells having different origin react in a different manner to the variations in architecture like topographies and pore features [92-93]. The stiffness of the scaffold material used for making scaffolds has an influence on the cellular activity [94-96]. All these properties for a particular scaffold can be studied only

by conducting various mechanical testing experiments on the materials of interest. Mechanical analysis of the scaffold is necessary apart from studying its degradation characteristics because the tissues that the scaffolds are going to replace possess varied mechanical properties and characteristics depending on the function they perform based on their location in the human body [40]. Typically for synthetic scaffolds, the mechanical analysis includes conducting compressive, tensile and cyclic tests.

2.5.1 Compression Test

This test is conducted to study the behavior of scaffold materials under extensive compressive loads. The material of interest is compressed followed by deformation under varying loads and the deformation values are recorded. Conducting this test is necessary because many tissues in the human body, e.g. cartilage in the elbow are subjected to extensive compressive loads during regular daily activities. Although this is important, this work only explored tensile test.

2.5.2 Tensile Test

This test is a basic test conducted on the materials. This is also called tension test. It often involves stretching the material of interest at a constant rate or until the material fractures or breaks.

An elastic material is one which snaps back to its original structure when the externally imposed strain or stress is removed. The stress-strain plot for the elastic

material shows a linear behavior (Figure 2.1). The elastic materials are found to follow "Hooke's Law". The slope of the line is called the Elastic Modulus.

$$Elastic\ Modulus = \frac{Stress}{Strain}$$

The stiffness of an elastic material is given by its Elastic Modulus value.

The stress-strain curve is linear until the point where Hooke's Law is applicable. After that point the material is no longer elastic and it exhibits permanent deformation. This region is called Plastic Region (Figure 2.1). This point is called the proportionality limit or the elastic limit for the material. In the plastic region the material is said to behave as a plastic material e.g. Polyether Terepthalate [97].

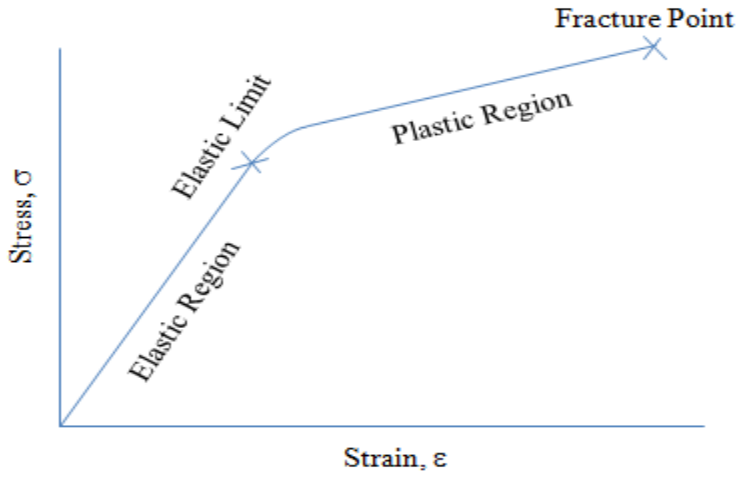

Figure 2.1. Stress-strain curve for a ductile material

2.5.3 Cyclic Test

Many day-to-day activities, eg. swinging of the arms and walking are repetitive in nature. Conducting cyclic test helps in better assessment of the mechanical behavior of

the tissues [19]. For conducting this test the material is first loaded to a predetermined level of stress and then the applied stress is removed. This process is repeated several times in a cyclic manner to mimic activities like the swinging of an arm.

All these tests do not completely describe the scaffold materials mechanical behavior. Majority of the tissues exhibit viscoelastic characteristics and hence it is important to study the viscoelastic properties of the synthetic scaffold material.

2.6. Viscoelasticity

Various tissues in the human body possess structures that are specific to the function they display like digestion, breathing, etc. The heart contains muscle tissues that help it to pump blood from and to all the other organs in the body. The fibrous tissue in the heart along with other tissues help in the regulation of the rhythmic beating of the heart [40]. All tissues exhibit viscoelastic and nonlinear elastic characteristics [98]. The human skin possesses viscoelastic properties [98]. The bone, which acts as a connective tissue is also modeled as an elastic material [99-100]. Similarly, cartilage which is another type of connective tissue is modeled as a quasilinear [101-102], linear [103-104], nonlinear [105] viscoelastic material [106]. Soft tissues like fascia, ligaments, nerves, blood vessels etc that encounter large deformations, are incompressible and also display nonlinear material behavior [2, 10-13]. These soft tissues rather than exhibiting pure elastic material behavior [14], exhibit viscoelastic property and they are also found to be anisotropic [15-18].

A material is said to possess viscoelastic property if it displays both elastic and viscous properties while stress is applied on them in order to deform them. Storing and dissipating energy later is one characteristic of viscoelastic materials. The other characteristics of viscoleastic materials include stress relaxation, hysteresis and creep [Figure 2.2]. Stress relaxation is seen in a material when it is subjected to constant strain rate over a particular period of time, held at that particular strain for a while and is finally relaxed once the peak stress is attained for that particular strain during the entire hold period. Hysteresis is the phase lag correlated to mechanical energy dissipation associated with the stress strain relationship for the material, which is subjected to constant loading and unloading. Creep can be explained as the material deformation when constant stress rate is applied. Creep can be thought of as the opposite of stress relaxation. Quite ideal, that stress returns to zero when strain returns to zero. If the film "gives" then returning to original zero strain requires compression.

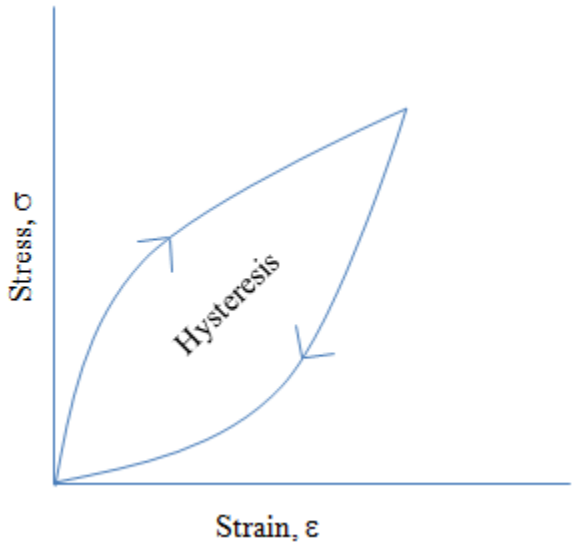

Figure 2.2 Stress-strain curve for a viscoleastic material

Many studies have been conducted to understand the viscoelastic behavior of scaffolds [5, 13, 107-109] but in order to understand the material mechanisms all these studies remain insufficient.

2.7 Viscoelastic Tissue Modeling Applications [1]

2.7.1 Biomechanics Applications

Biological tissues exhibit load-history-dependent and time-dependent mechanical behavior. Many soft tissues like tendons, muscles, fascia, nerves, synovial membranes ligaments, fibrous tissues, blood vessels, and fat undergo large deformations, are nearly incompressible, and display nonlinear material behavior [2, 10-13]. Biological tissues which are anisotropic are found to exhibit viscous and elastic behaviors [15-18]. Viscoelastic materials usually store and dissipate energy within multi-component complex molecular structures; producing hysteresis and they also allow stress relaxation and creep to occur. A full description of the mechanical response of the materials requires multi-component, nonlinear, viscoelastic behavior.

2.7.2 Surgical Simulator Applications

Image-guided surgery improved the recovery time, decreased trauma and reduced health care costs significantly. Also, robotic surgery has helped in precise localization of the target and has also helped in dissection without much of damage [110]. Soft tissue navigation involves a very complex process because of its high potential of damage. Simulation technologies have been developed in order to train new generation surgeons

[111]. Surgical simulators were developed provide haptic feedback and realistic visuals for effective surgeon training. However, for proper development of reality simulators a valid soft tissue viscoelastic model is required. In order to develop models accurate description especially of the biomechanical characteristics of tissues is required. During regular physiological function various organs such as large intestine, skin, small intestine, stomach, liver, and spleen are subjected to extensive stress-strain loads. However, at the time of surgery, they are subjected to different loading conditions. Viscoelastic modeling of tissue structures is required for conducting less invasive surgery and also to develop surgical robots [112]. Hence understanding the mechanical behavior of the organs is necessary.

2.7.3 Tissue Engineering Applications

Development of prosthetic devices for diseased tissue replacement is increasing. Similarly tissue regeneration to address the scarcity of available tissues is also increasing. Biodegradable scaffolds are developed in order to account for the above requirements. The developed scaffolds should match and satisfy the mechanical properties of native tissues. In order to do this the viscoelastic behavior of tissues should be understood.

2.8 Viscoelastic Models

Viscoelasticity of the soft tissues were quantified using various models like the Voigt, the Maxwell and the Simple Linear Models [113]. Dominating the bioengineering

literature of viscoelastic tissue models is the Quasi Linear Viscoelastic (QLV) modeling approach published by Fung [3] in 1967.

2.8.1 Quasi-Linear Viscoelastic (QLV) Model [1]

QLV theory developed by Fung [3] assumed that for soft tissues, the instantaneous stress that results on the application of a ramp strain can be expressed as:

$$\sigma(t) = G(t) * \sigma^{e}(\varepsilon) \tag{2.1}$$

Where, a convolution integral of the stress relaxation function was used to express the stress relaxation behavior. The convolution integral ("*") is given by

$$\sigma(t) = \int_{-\infty}^{t} G(t-\tau) \frac{\partial \sigma^{e}(t)}{\partial \varepsilon} \frac{\partial \varepsilon}{\partial \tau} d\tau \tag{2.2}$$

where σ(t) is the stress at any given time instant, the reduced relaxation function is represented by G(t), the strain history is represented by $\frac{\partial \varepsilon}{\partial \tau}$ and $\sigma^{\varepsilon}(t)$ stands for the instantaneous elastic response (the maximum stress that is in accordance with a strain ε which is given as an instantaneous step input). The function G(t) stands as the stress response of the soft tissue which is time-dependent and normalized by the same stress that is present when strain is applied as step input. Practically, while conducting tests, it is considered that the applied strain history begins from time t=0. Hence, Equation. (2.2) is rewritten as

$$\sigma(t) = \int_{0}^{t} G(t-\tau) \frac{\partial \sigma^{e}(t)}{\partial \varepsilon} \frac{\partial \varepsilon}{\partial \tau} d\tau \tag{2.3}$$

Fung, for the case of soft tissues introduced a generalized G(t) function equation which has the form

$$G(t) = \frac{1 + C\left[E_1\left(t/\tau_2\right) - E_1\left(t/\tau_1\right)\right]}{1 + C\ln\left(\tau_2/\tau_1\right)} \tag{2.4}$$

where C is a dimensionless parameter of the material that represents the magnitude of viscous effects that are present. The fraction of relaxation is also related to C. The time-constants are represented by τ_1 and τ_2. They demark the limits of the long and short-term soft tissue material responses. Equation (2.4) represents G(t) as constructed on a continuous spectrum of soft tissue relaxation. The exponential integral function, $E_1(t/\tau)$ is of the form

$$E_1(t/\tau) = \int_{t/\tau}^{\infty} \frac{e^{-z}}{z} dz \tag{2.5}$$

If there is sufficient time between τ_1 and τ_2 that $\tau_1 << t << \tau$ [23] , or if 1 sec is the time duration [15], then Equation. (2.4) can be modified as

$$G(t) = \frac{1 - C\gamma - C\ln\left(t/\tau_2\right)}{1 + C\ln\left(\tau_2/\tau_1\right)} + \mathrm{O}(0) \tag{2.6}$$

where γ stands for the Euler constant. The value of γ is 0.5772. If the cumulative value of the terms that belong to the infinite series is small, which is represented by O(0), they can be neglected.

Hence,

$$G(t-\tau)=\frac{1-C\gamma-C\ln\left(\frac{t-\tau}{\tau_2}\right)}{1+C\ln\left(\tau_2/\tau_1\right)} \tag{2.7}$$

Abramowitch and Woo [20] for modeling the collateral ligament that possessed viscoelastic behavior used QLV modeling as the basic. In their model the instantaneous stress response was represented by an exponential approximation [19, 23]

$$\sigma^e(\varepsilon)=A\left(e^{B\varepsilon}-1\right) \tag{2.8}$$

where *A* stands for the elastic stress constant which has units of stress (MPa), and *B* stands for the elastic power constant which is dimensionless.

Toms, *et al.* [22] used an alternative stress relaxation function which was referred to as the Modified Quasi Linear Viscoelastic Model (MQLV). In their model, the reduced relaxation function ,G(t) was defined as

$$G(t)=ae^{-bt}+ce^{-dt}+ge^{-ht} \tag{2.9}$$

where a, b, c, d, g and h represent the parametric constants. The analytical solution is as shown in [114].

For both the models, nonlinear regression was used to determine the values of parametric constants. Typically in the literature for regression to obtain model coefficient values, one of several algorithms available from Excel Solver or a Levenberg-Marquardt algorithm, with the code written in either Mathematica or Matlab or other similar software packages is used .

Unfortunately, several aspects of the QLV model prove the model to be inapplicable to the nonstationary, nonlinear and confounding aspects of the viscoelastic deformation and relaxation mechanisms of biological tissue structure [4-9].

2.8.2 Criticism of Current Approaches to Viscoelastic Modeling.[1]

The criticisms to the current approaches were as follows:

1. Equation (2.8) is nonlinear. This violates the linear requirement condition of the convolution integral. Most of the work seen in the current approaches proves to be mathematically internally inconsistent.
2. Assumptions used in Equation (2.6) to truncate and eliminate terms need to be verified after regression determines the model coefficient values. Validation of the regressed parameter values could not be seen in literature.
3. The G(t) in Equation (2.4) assumes continuous spectrum of relaxation time-constants, but none below τ_1, and none above τ_2, and an exponential population distribution in between. The stress relaxation function of [17] provides solutions that are tractable. Although these composite relations may be right, they take into account certain fundamental assumptions about the soft tissue material, which need to be verified.
4. The shrinking cross-sectional area of the sample which ought to be included is not included in the QLV approach.
5. The model parameters A, B, C, τ_1, and τ_2 do not have a direct relation between molecular structure and physical meaning. For example, a material cannot be designed with a particular τ_2 value.

6. The QLV approaches model viscous behavior that result in permanent deformation but do not model a material that deforms when stressed and relaxes back to its original dimensions on removal of the stress.
7. Although the G(t) function of Equation (2.6) takes into account the range of relaxation rates, that result from a range of stress relieving mechanisms, each of these mechanisms is accepted as possessing the same instantaneous σ/ε curve.
8. The derivation for the models necessarily start loading from a relaxed stress-free state which precludes using the model developed for a subsequent strain after a partial relaxed period.

2.8.3 Criticism of Current Approaches to Determine Model Parameter Values

A basic problem encountered in the least squares regression approach for nonlinear functions is the major difficulty in finding the global optimum for the objective function as the function may have multiple local optima that completely divert or trap searches. It can be clearly seen that the solution obtained significantly depends on the initial guesses. Further, the appropriate values for regression stopping criteria on the objective function (SSD), decision variables (model parameters), or their time increment needs an *a priori* knowledge of the data-equation system. Hence the model parameter values that result from nonlinear regression largely depend on the intital user choices, which mostly appear inconsistent within the literature.

2.9 Optimization

Another problem associated with modeling is the optimization stage. Research reports difficulty in optimizing viscoelastic model parameter values to best match the model with experimental stress-strain-time data. There are multiple local optima for the objective statement, and approaches to the minima are often exasperatingly slow (even with classic best practice nonlinear optimizers such as Levenberg Marquardt). Further, optimization must include constraints on the parameter values, suggesting that direct search methods may be more appropriate than gradient based methods. Accordingly, techniques such as best-of-N [30] starts and direct search techniques have been investigated for determining the probable global optimum subject to multiple constraints. The applicability of emerging optimization techniques for model parameter adjustment is explored along with new regression approaches.

A new optimization technique called Leapfrogging is also explored [31]. Test cases on this technique revealed that this technique gave better optimized values when compared to other techniques with fewer number of function evaluations [31].

Since there are multiple optima in this high dimensional nonlinear search, the optimizer is run for "N" times from a random set of initial model coefficient values. The value of "N" should be chosen properly in such a way that it is not too small that the optimizer is not able to capture the best model coefficient values within that range and not too big that the optimizer takes more time to get the best model coefficient values increasing the computational burden. Hence an appropriate value for the "N" should be calculated. The value of "N" is calculated [30] so that the best set out of the N results within the user defined probability stands as one of the best sets of model parameter

values out of all possible solutions. During each trial, out of the "N" trials the optimizer stops when there is no significant improvement statistically in the objective function, i.e. minimizing the sum of squared deviation of the model from the experimental data, relative to variance in the data [115-116]. Most of the optimization problems use a specific change in the decision variable or a specific change in the objective function as stopping criteria. But they require a prior knowledge of the objective function and are infected by human prejudice. Hence, this work uses a steady-state stopping criteria which observes sum of squared deviation of model data from experimental data, from a random subset at each iteration and stops when there is no statistical improvement in the sum of squared deviation with respect to inherent variability between data and model.

CHAPTER 3

APPROACH

3.1 Modeling [1]

Tissue stress relaxes in time under constant strain, and tissue shape progressively deforms under constant load. Also, portions of the internal structure of tissues gradually return toward the original structure when external stress or strain is relieved. Because of all these reasons stated above time-dependent viscoelastic models are required. The time-dependent behavior also depends on the stress-strain history. Further, since tissues are comprised of several participating structures (cells, matrix, fibrils, etc.), each having individual mechanisms; a multi-component, viscoelastic model is required. Further, since tissue properties are not constant; nonlinear, multi-component, viscoelastic models are required. Finally, since many tissue components do not relax fully to the original internal structure, the commonly employed dashpot element (which lets the spring return to zero stress) is inappropriate. New constitutive relations are required for the nonlinear, multi-component, viscoelastic models.

This work will demonstrate the validity of appropriate nonlinear viscoelastic relations and a pseudo-component approach for modeling the complex tissue structures. Six composite model types developed using various combinations of the pseudo-components are used to examine the consistency of the composite model with

experimental data. The composite models are developed using a combination of a hyper-elastic spring or a spring-and-dashpot model along with total-relax-back-to-original structure or retain-the-as-stretched structure.

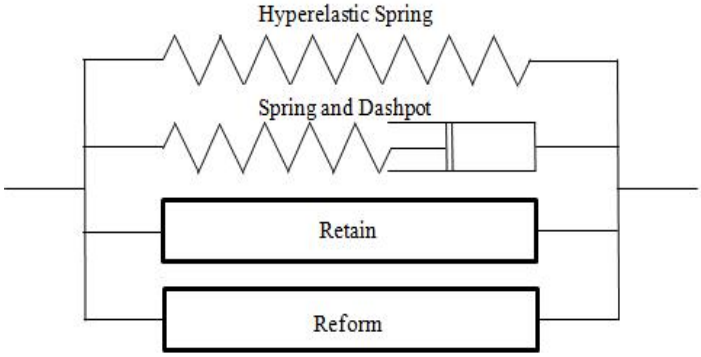

Figure 3.1: Pseudo-Components

The four pseudo-components used in this study to develop the composite models are shown in Figure 3.1. The 6 composite models identified as best for the tissues used in this study are developed from various combinations of 2 or 3 of these 4 components.

3.1.1 Pseudo-Component Model Components [1]

Although relaxation begins as soon as stress is applied, and continues until stress is relieved, the following illustration will separate the stages (externally applied stretching and internal relaxing) for convenience and clarity of communication. The subsequent mathematical analysis will treat the two phenomena simultaneously.

Consider a material with zero internal stress at rest that is not stretched (Figure 3.2a). Let the length of the original film be L_0 with height H_0 and width W_0. Viscoelastic

components are those that are represented by line segments that are randomly oriented and demonstrate that the orientation is at a stress-free state. The line segments are termed "components" which symbolizes a general category of functional relationships. For example, a line segment in a macromolecule could represent folded sections, which in response to strain could become unfolded.

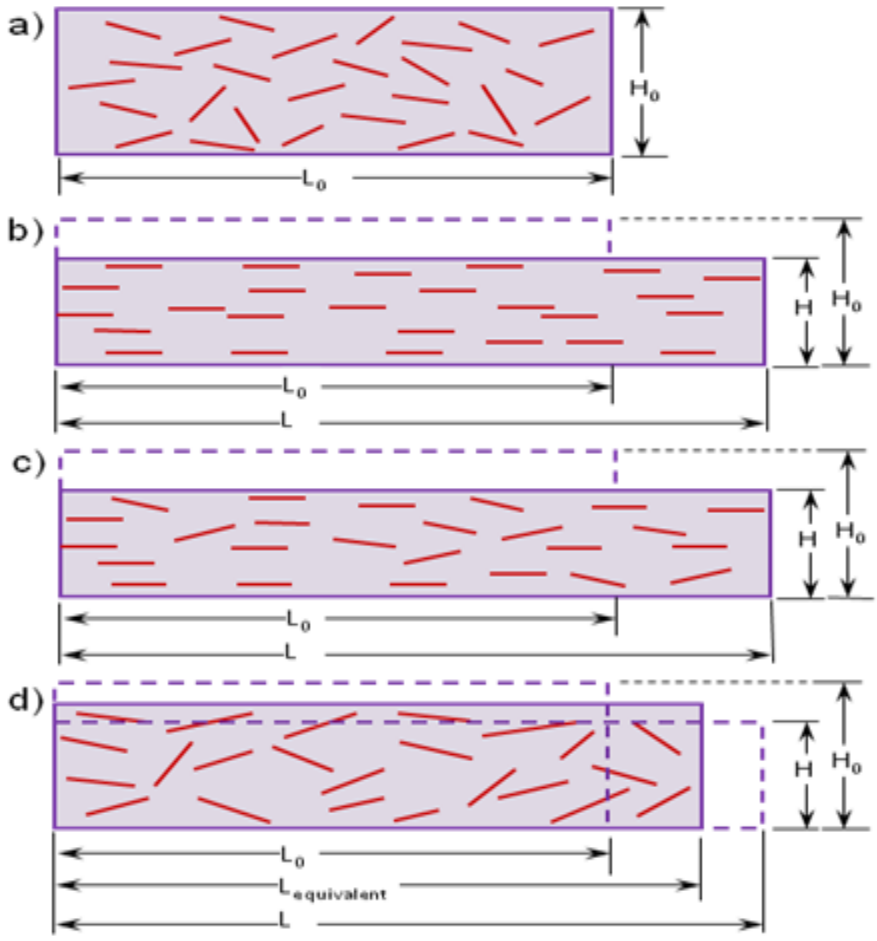

Figure 3.2. Viscoelastic Stress relaxation concept (a) material at rest (b) material elongated and stressed (c) material elongated and held while stress partially relaxes and (d) material realeased.

When strain stretches the folded section as a result of application of external deformation, internal stress is created. The stretch in the folded section is represented as aligned components (Figure 3.2b**)**. The new length is now $L=L_0*(1+\varepsilon)$, and if the volume of the material remains the same, the lateral contraction creates new width and height of W and H respectively. The stress can be determined as, $\sigma_0 = F/(H_0*W_0)$ where F is the tensile force while ε represents the strain. If held at length L, the stresses on the folded sections may cause them to unfold, partially alleviating the stress. The unfolding may happen over time, as thermal motion permits, providing progressive relaxation to the new deformed state, as illustrated in Figure 3.2c.

Thermal processes may lead to refolding when the external deformation is removed. (Figure 3.2d). This leads to a permanent elongation in the length of the film represented as $L_{equivalent}$ (equilibrium length) but with the original random, stress-free structure.

The four pseudo-components shown in Figure 3.1 are discussed below.

Pseudo-component 1: (Hyper-elastic Spring): This component characterizes the material in such a way that it does not relax internal stress. According to this component the material rebounds to its original structure and size on removal of external load. This component has a nonlinear stress response to the strain as shown in Figure 3.3, curve (a) or (b). If the stress-strain curve is linear, the material would be a classic Hookean elastic material.

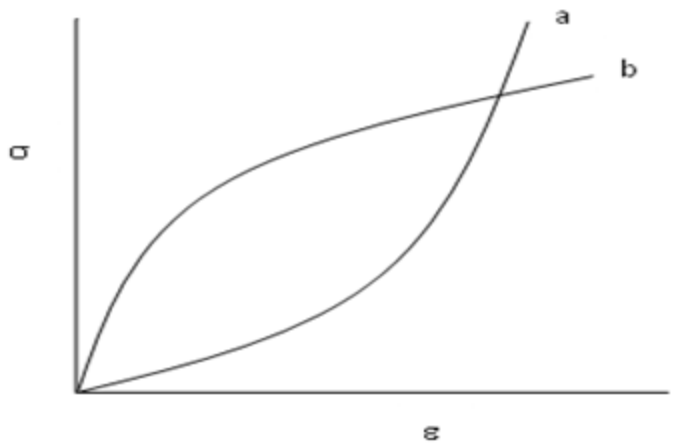

Figure 3.3: Stress to strain relation of a hyper-elastic spring

Pseudo-component 2: (Spring-and-Dashpot): This component does not account for the necking in of the material i.e. it does not account of the changes in W and H of the material when the length changes due to elongation. When held in an elongated state, the dashpot elongates and the spring returns to its original stress-free state (length).

Pseudo-component 3: (Reform): As opposed to the spring-and-dashpot component, this component accounts for the necking in of the material i.e. it does account for the changes in W and H of the material when the length changes due to elongation. Partial reformation of the components in the material to their original orientation (Figure 3.2c) happens while the elongated material is held at length L. Prior to total relaxation if the external loading is removed, the material restores itself to an elongated state which is permanent (Figure 3.2d), which has the same internal structure as the original zero stress random orientation state. $L_{equivalent}$ is the permanent elongated length. Since the volume of the film is a constant and since the film original length L_0 is lesser than $L_{equivalent}$ (L >

$L_{equivalent} > L_0$), the cross section area at this point is smaller than the original cross sectional area of the film. Yet, if the strain in Figure 3.2c when partial relaxation occurred, is not relieved, the expected stress would be that if the sample of original length, $L_{equivalent}$ had been elongated to L. The strain would be $(L-L_{equivalent})/L_{equivalent}$. Although there would be a distribution of orientations and unfolding kinetics, the pseudo-component will be modeled as having average behavior. In the fully relaxed state, these components are oriented in a random fashion similar to the original sample. Once again when strain is applied it leads to the same stress response identical to that of the original sample, but with a lower cross sectional area. The reform component in Figure 3.4 explains the stress behavior after the tissue material is relaxed according to this concept. Once the material undergoes total relaxation, it should have returned to its original stress-strain orientation, and the reform in Figure 3.4 shows that there is right translation from the near-origin section where the impact of subsequent strain on subsequent stress will be as though the stress were starting completely fresh.

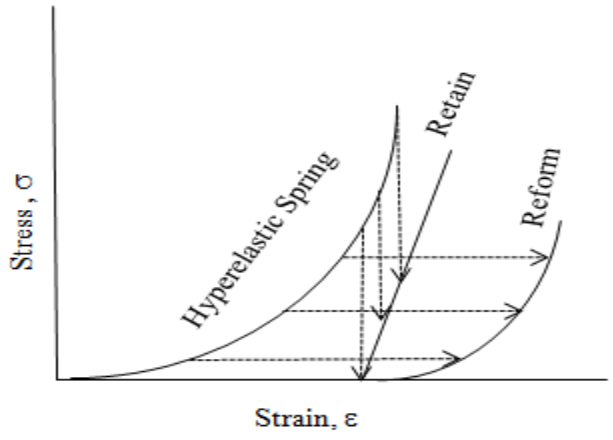

Figure 3.4: Conceptual illustration of Hyper-elastic spring, Retain and Reform component

Pseudo-component 4: (Retain): Like reform, retain also accounts for the necking in of the material because of reduction in cross-sectional area when the material is elongated. However, here, the material components retain the orientation that resembles a stretched orientation when the material is held at an elongated length, L. By arranging itself to a new structure orientation the material components relieve its stress. Even after relaxation occurred, if the application of strain is continued, the pattern for the stress will persist from the newly oriented structure. The retain component in Figure 3.4 explains the stress behavior after the tissue material is relaxed according to this concept. Figure 3.4 shows that subsequent strains act from the previously strained point.

Combinations of these 4 pseudo-components are used to build composite models.

3.1.2. Composite Models

Each of the composite models describes a structure in which the pseudo-components are acting in parallel (Figure 3.1). There are two aspects of the models that are needed to completely describe each of the composite models. One aspect describes the number of parallel pseudo-components that make up the composite model. The second aspect describes the type of each pseudo-component. Combined, the number of pseudo-components and the behavior of each is termed the model architecture. In the initial investigations of Mirani [40] and Kornkorn [32] several basic architectures were studied. Four types of Architectures are investigated in this work.

Architecture A) 8 parameters – This structure has 4 elements set up in parallel where in one of those is a nonlinear spring and the rest all are linear spring-and-dashpot

components.

Architecture B) 9 parameters – This structure has 3 elements in parallel each of which is a viscoelastic pseudo-component. In this architecture screening the viscoelastic components are all retain.

Architecture C) 8 parameters – This structure has 3 elements in parallel out of which one is a nonlinear hyper-elastic spring while the other two are viscoelastic pseudo-components. In this Architecture screening the viscoelastic components are all retain components.

Architecture D) 11 parameters – This structure has 4 elements in parallel one of which is a hyper-elastic spring and the others were viscoelastic pseudo-components. In this Architecture screening the viscoelastic components are all reform components.

Two criteria are used to select the best architecture. They are 1) the sum of squared deviations (SSD) of the model predictions from the experimental data, and 2) simplicity of the model. Architecture A, even though it had 4 pseudo-components, was limited by linear stress-strain relations and could not capture the experimental stress data as well as the other three architectures. Architecture B, regularly showed a very high τ (time constant) value for one component, which signifies that out of the three, one of the retain components did not relax, which in turn implies that it acts as a hyper-elastic spring. Architecture C explicitly uses a hyper-elastic spring as one pseudo-component achieving identical best fit as architecture B, but with one fewer parameter. Architecture D did not improve the fit to data relative to the undesired aspect of increasing the number of adjustable parameters. Accordingly, Architecture C as best and variations on it are selected for this work.

Within Architecture C, one pseudo component is a hyper-elastic spring, and the other two would be the 6 permutations of Pesudo-Components 2, 3, or 4 as follows:

Composite Model 1: One hyper-elastic spring with two spring-and-dashpot components.

Composite Model 2: One hyper-elastic spring with two reform components.

Composite Model 3: One hyper-elastic spring with two retain components.

Composite Model 4: One hyper-elastic spring with one retain and one spring-and-dashpot component.

Composite Model 5: One hyper-elastic spring with one reform and one spring-and-dashpot component.

Composite model 6: One hyper-elastic spring with one reform and one retain component.

3.1.3. Mathematical Statement [1]

It is important that a mathematical statement is formulated for the composite models developed. Figure 3.3 symbolizes for a pseudo-component an instantaneous nonlinear stress-strain relation which is modeled as,

$$\sigma_i = A_i(e^{B_i\varepsilon_i} - 1) \tag{3.1}$$

where "i" (subscript) represents the i^{th} pseudo-component. In this equation the coefficients A and B must have the same sign. In Figure 3.3, Curves a and b illustrate the plot when A,B < 0 and A,B > 0 respectively.

Also, as far as this work is concerned each of the viscoelastic pseudo-component undergoing internal material deformation are modeled as having their rate of internal

stress relaxation of the order 1, which at infinite time tends towards complete relaxation of zero stress. The relaxation model with no strain-rate-induced stress is,

$$\tau_i \frac{d\sigma_i}{dt} + \sigma_i = 0, \sigma_i(t = 0) = \sigma_0 \tag{3.2}$$

As Figure 3.1 represents the material with internal deformation concept Equation (3.1) is the stress model when instantaneous strain at one stage is applied and the stress relaxation is revealed by Equation (3.2) if the soft tissue is held elongated for a period of time. Yet, when the material is relaxing, if it is strained at a particular rate, then derivations done rigorously enumerate that Equation (3.2) should also include the injection of internal stress at that particular rate, which happens as a result of the rate of external strain.

$$\tau_i \frac{d\sigma_i}{dt} + \sigma_i = \tau_i \frac{\partial \widehat{\sigma}_i}{\partial \varepsilon} \frac{d\varepsilon_i}{dt} = \tau_i A_i B_i \exp(\, B_i \frac{Lequ_i}{L} \varepsilon\,) \frac{Lequ_i}{L} \frac{d\varepsilon_i}{dt},\ \sigma_i(t = 0) = \sigma_0 \tag{3.3a}$$

$$\tau_i \frac{d\sigma_i}{dt} + \sigma_i = \tau_i \frac{\partial \widehat{\sigma}_i}{\partial \varepsilon} \frac{d\varepsilon_i}{dt} = \tau_i A_i B_i \exp(\, B_i \varepsilon\,) \frac{d\varepsilon_i}{dt},\ \sigma_i(t = 0) = \sigma_0 \tag{3.3b}$$

Equation (3.3a) is for the reform part of the recovery of stress of the internal structure, Equation (3.3b) is for the retain part which allows a stress relief. Equation (3.3a) is analogous to the spring-and-dashpot model owing to the term for reformation of the spring is allowed whereas Equation (3.3b) is not similar to spring-and-dashpot model, because of the fact that the "spring" cannot return to the state of zero elongation.

Numerical methods can be used to solve Equations (3.3a) and (3.3b), and then any stress or strain history can be modeled. The stress of pseudo-component "i" (Equation (3.3a)) which is partially relaxed, at the completion of a Δt time increment, the strain-equivalent on the film component can be determined by the inverse of Equation (3.1)

$$\varepsilon_{equ,i}\,(t+\Delta t) = \frac{\ln\left(\frac{\sigma_i(t+\Delta t)}{A_i}+1\right)}{B_i} \tag{3.4}$$

Equation (3.4) gives the value of strain-equivalent for a pseudo-component using which the equivalent length is calculated as

$$\mathrm{L_{equ,i}(t+\Delta t) = L_0(1+\varepsilon_i(t+\Delta t))} \tag{3.5}$$

The sample length at the next time instant, *t*, can be calculated from experimental strain, ε_0 as

$$\mathrm{L(t) = L_0(1+\varepsilon_0(t))} \tag{3.6}$$

and hence the new strain that is effective on the pseudo-component is

$$\mathrm{\varepsilon_i(t) = \frac{[L(t)-Le_{equ,i}(t)]}{L_{equ,i}(t)}} \tag{3.7}$$

For each pseudo-component the stress vs. time is modeled by sequential application of Equations (3.3a), (3.6), (3.7) or (3.3b), (3.4) and then (3.5). As numerical methods are used to solve equations *Δt* should be small relative to the time-constants and the time periods taken for the corresponding changes in strain rate. This work uses Euler's method for which *Δt* should be less than about one-tenth of the smallest time constant.

Here, it should be noted that the measurement obtained as a result of tensile test experiment is not tensile stress but tensile force though the tensile tests report stress. The tensile force obtained here is represented as the sum of all forces attributed to each of the pseudo-components.

Assuming that each of the pseudo-components retain a volume that is constant

upon deformation, and the contraction in each of the dimensions is uniform, and the length of the material *L* is long enough that the geometric end effects due to the clamping of the sample could be eliminated, the extension in length due to strain causes the cross-sectional area to reduce to

$$\mathrm{A} = \frac{\mathrm{A_0}}{(1+\varepsilon_0)} \tag{3.8}$$

If for an i[th] pseudo-component having a representation as Equation (3.3a) and if it is relaxed to the equivalent length, the "original" area that is unstressed is

$$\mathrm{A} = \frac{(1+\varepsilon_\mathrm{i})\mathrm{A_0}}{(1+\varepsilon_0)} \tag{3.9}$$

Hence the force due to the stress on i[th] pseudo-component of Equation (3.3a) will be,

$$\mathrm{F_i} = \sigma_\mathrm{i}\mathrm{A_i} = \frac{(1+\varepsilon_\mathrm{i})\sigma_\mathrm{i}\mathrm{A_0}}{(1+\varepsilon_0)} \tag{3.10}$$

The measured stress is determined by volume weighting using the volume fraction $\emptyset_\mathrm{i}$ and the ratio of sum of the forces due to each of the pseudo-components to the original area A_0,

$$\sigma_{composite}(t) = \sum_{i=1}^{N} \frac{\emptyset_i \sigma_i(t)(1+\varepsilon_i(t))}{(1+\varepsilon_0(t))} \tag{3.11}$$

where "N" stands for the total number of pseudo-components

It would seem that the volume fraction, $\emptyset_\mathrm{i}$, and the stress-amplitude factor, $\mathrm{A_i}$, from Equation (3.1) are independent model parameters. However, when Equation (3.11) is written in terms of strain only, the two coefficients appear as a product.

$$\sigma_{composite}(t) = \sum_{i=1}^{N} \frac{\emptyset_i A_i\left(e^{B_i \varepsilon_i(t)}-1\right)(1+\varepsilon_i(t))}{(1+\varepsilon_0(t))} \tag{3.12}$$

Experimental stress-strain-time data cannot separate the functionality of $\emptyset_i$ and A_i. Accordingly, the model coefficients that characterize the viscoelastic properties of each pseudo-component that are adjustable in the "AB" material will be the $\emptyset_i A_i$ product, B_i, and τ_i. If the pseudo-components are identified and volume fractions are known, then τ_i , A_i , and B_i would be the adjustable model coefficients. However, the pseudo-component is not meant to represent one particular component, but the collective behavior of the integrated whole. This work proposes τ_i, the $\varphi_i A_i$ product, and B_i as the adjustable model coefficients. For convenience the $\varphi_i A_i$ term will be shortened to just A_i.

At each time step, Δt, Equation (3.11) will provide the value of the superficial stress measured on the composite. One major asset of this time-incremental, numerical model vs. an analytical integrated model, is that for the time-dependent behavior rate of strain there are no assumptions. The computational algorithm using numerical model is not changed even when the strain rate is started, stopped, changed, or re-started. Accordingly the same model could be used for compression, and either cyclic or sequential stress or strain loading. Further, it is a simple task to replace the instantaneous stress-strain relation of Equation (3.1) and its inverse of Equation (3.4) with another relation, and to also not violate the convolution integral requirements in often-used viscoelastic models.

In order to determine values of the model parameters that are adjustable, least squares regression using $\sigma(t)$ and $\varepsilon(t)$ data and the pseudo-component model that is numerically-solved to predict the measured stress of the composite models will be used.

3.2 Optimization

3.2.1 Objective Statement

Quantifying the viscoelastic behavior of PLGA, PCL, SIS is important. Optimization techniques are used for the quantifying this process. The objective statement for optimization is to minimize the deviation of the model data points from the experimental data points. The deviation is calculated as sum of square of the deviation (SSD) of the model from the experimental value.

$$SSD = \sum(\sigma_{experimental\ data} - \sigma_{model\ data})^2 \quad (3.14)$$

3.2.2 Decision Variables

The decision variables i.e. the variables that are free to change in order to accomplish the objective statement are the model parameters of the Equation 3.12 namely A_1, B_1, A_2, B_2, τ_2,A_3,B_3 and τ_3

3.2.3 Optimizers

An algorithm is written in Excel/Visual Basic for the optimizers to accomplish stated/required the objective statement. The optimization techniques used are as follows:

Cyclic Optimization Technique [117]: Cyclic optimizer belongs to the direct search class of optimizers. It evaluates the objective function value at every trial and does not require the value of the derivatives. This optimization technique was developed by Dr. R. Russell Rhinehart. This optimization technique involves the usage of heuristic factors. It

explores one DV at a time. During every new trial the optimizer moves forward expanding the step size of the decision variables if the direction of movement is towards the minimum, else it will reverse its direction and start contracting the step size of decision variables until it finds the correct direction. This technique takes one step at a time. The step may be either keeping or returning to the base case. It ultimately cycles through each DV. This algorithm for this optimization is simple to understand and is robust.

Rhinehart modified Levenberg Marquardt Optimization Technique [117]: Levenberg-Marquardt optimization technique is one of the most widely accepted, balanced, and used optimizer. It is an efficient and robust optimizer. Levenberg-Marquardt method uses Incremental Gradient (or Incremental Steepest Descent) method and as the minimum is approached it switches to Newton's method. In order to define a smooth switch between the two methods, a scalar multiple [λ] of the identity matrix was added to the hessian matrix defined for the Newton's method.

For Incremental Steepest Descent method the incremental step size for the decision variable is defined as:

$$\underline{\Delta DV} = -\alpha \underline{\nabla} f_0 \tag{3.14}$$

Where $\alpha = \frac{1}{\lambda}$ is a scalar that defines the step size that the DV should take when it jumps from the previous DV value to the present, $-\underline{\nabla} f_0$ is the negative gradient of the function which points in the direction of steepest descent.

Newton's method uses the Hessian and the negative gradient to calculate the incremental step size as:

$$\underline{\Delta DV} = -\underline{\underline{H_{f_0}^{-1}}}\,\underline{\nabla} f_0 \tag{3.15}$$

Where $\underline{\underline{H_{f_0}^{-1}}}$ does two things adjusting the steepest descent direction to aim at a minimum and also determine the correct step size in order to jump to the minimum.

Hence Levenberg- Marquardt is defined as:

$$\underline{\Delta DV} = -[\underline{\underline{H}}(f) + \lambda \underline{\underline{I}}]^{-1}\underline{\nabla} f_0 \tag{3.16}$$

Where λ is the scalar multiplier to the identity matrix.

When λ is large Equation (3.16) becomes an Incremental Steepest Descent method and when λ is small it becomes Newton's method.

The choice of λ is important for this method. The Levenberg Marquardt rules on the scalar are that whenever the movement is success it becomes half its original values in order to switch to Newton's method and becomes twice its original value whenever the movement is a failure. The drawback of this method is choosing the scalar value because the effective use of this method depends on the order of magnitude of second order derivatives of the objective function in comparison to the scalar identity matrix. Also, the choice of the scalar depends on the second derivatives which are not easily seen. Influence of Incremental Steepest Descent or Newton's method depends on the λ value and it either may make the optimization technique proceed to a minimum at a very slow rate due to more influence by Incremental Steepest Descent method or the optimization technique may find a maxima or saddle point due to higher impact of the Newton's method which is based on making the numerical values of the derivatives zero. The choice of the scalar is scale dependent. It may turn out to be too small or too large

depending on the Hessian elements. Hence, Dr. R. Russell Rhinehart modified the Levenberg-Marquardt technique to Rhinehart modified Levenberg-Marquardt (RLM) Technique.

RLM1: The first modification for the Levenberg Marquardt optimization technique initially tests the selected DV by λ-weighted Incremental Gradient and Newton-Raphson (IGNR) method. In this technique, as opposed to Levenberg Marquardt method instead of using a high λ value, the Incremental Gradient method is weighted by λ and Newton-Raphson by (1-λ) where $0 \leq \lambda \leq 1$. If this gave a better objective function value, then the optimization technique accepted the IGNR result as the new base case and reduces λ so that it starts following the Newton-Raphson method. If the optimization technique gave a bad objective function value compared to the base case, then λ value was increased making it to follow the Incremental Gradient (IG) method. The Incremental Gradient trial solution is then tested. If IG is better than the base case then the step size for IG is increased or else it is decreased.

RLM2: In this version both IGNR and IG are simultaneously tested and the λ value is varied depending on which method gives good objective function and which gives bad objective function. This version was considered for this study.

RLM3: This version is similar to version 1 but has two enhancements. 1) It uses scaled variables for the steepest descent calculation so that the calculation becomes dimension independent. 2) Uses an attenuation factor to either temper or accelerate the Newtonian action.

RLM4: This version uses IG and Newton-Raphson search algorithm alternately. This optimization technique chooses the method that gives the best objective function value as the new base case and proceeds appropriately.

Leapfrogging [31, 117]: This technique starts with a set of players (trial solution) located randomly in the decision variable space. Each set of players acts as a swarm of particles. This technique relocates the position of the players by randomly reflecting the player with the worst objective function value across the player with the best objective function value at each iteration on an average half the distance from the player with the best objective function value. The basic driving philosophy for Leapfrogging is eliminating the decision variable values that give the worst objective function value. This method is robust and efficient in finding the minima.

3.2.4 Multi Start Criterion [30]

It happens most of the time that the optimization algorithms get stuck at local minima. In order to find the global minima, it is necessary that the optimizer search is initiated multiple times. The performance of the optimizer is decided on the SSD value (objective function) that it returns for each trial. In order that the optimization technique selects the best model parameter values so that it returns the best objective function it is important that the number of trials from random intializations is large enough. The VBA algorithm used for each of the optimizers is developed in such a way that each of the new trial starts with a random set of initial decision variable values. The number of initial trials required is given by the formula developed by [30] as

$$N = \frac{\ln(1-c)}{\ln(1-f)} \tag{3.17}$$

Equation (3.17) gives the number of trials that is required for the desired probability (c) of atleast 1 of N reaching an optimum which represents the desired best fraction, f, of all possible solutions.

3.2.5. Stopping Criterion [40, 116]

A suitable stopping criterion is incorporated in the optimizer algorithm. Stopping criterion is to stop the optimization technique, its process, for each of the random set of initial values/guesses for the DV(s). Commonly, a convergence criterion is included to stop the optimizer or a overriding criterion is set so that the optimizer is made to stop whenever the number of trials exceeds a threshold value. There are several classic approaches to stopping criteria. The only best way to judge whether the stopping criterion is too severe or too lenient is to observe the results obtained. An *a priori* knowledge about the function, its behavior and the behavior of the optimizer is required to select suitable stopping criteria.

The stopping criterion employed in here is that the VBA code randomly selects a subset (RS) of model data for each iteration and calculates the root-mean-squared (RMS) deviations and terminates the optimization technique when the RMS-RS [115-116] value shows no major improvement with iteration number. There are several advantages associated with this stopping criteria technique. This stopping criteria technique is single criterion and scale-independent. Also, this technique does not require any kind of user-chosen thresholds. There are ample number of ways to analyze the data for probable

steady state and transient conditions. This stopping criteria method terminates each of the iterations depending on a preset ratio of variance value, an R-statistic as measured on the same set of data. At steady state the expected value of the R-statistic is 1. However, a near steady state situation could generate a lower R-statistic value < 1. So to be sure that the optimizer has converged, that there is no further improvement possible, that the RMS-RS value is at steady state, an R-statistic value of 0.8 is used [118].

CHAPTER 4

EXPERIMENTAL

4.1 Composite scaffold generation [32, 40]

Composed scaffolds were developed based on the concept that a blend of natural polymers with synthetic polymers resulted in superior quality scaffolds that were better than natural polymer scaffolds or synthetic polymer scaffolds individually. Poly Lactic and Glycolic Acid (PLGA), Poly Caprolactone (PCL) and Sub Intestinal Sub mucosa (SIS) are the composite scaffolds considered for this work.

4.1.1. Materials

1) PLGA

For generating polymer samples of Poly Lactic and Glycolic Acid (PLGA) composite scaffolds, two of the materials namely 50:50 (lactic and glycolic acid) PLGA polymer pellets along with ester terminated (nominal) with 90-120 kDa molecular weight (Mw), were purchased from LACTEL Absorbable Polymers (Pelham, AL). Gelatin type – A (300 Bloom) and Chitosan (200-300 kDa molecular weight (Mw), 85% DD) were purchased from Sigma Aldrich Chemicals (St. Louis, MO), Aaper Ethyl Alcohol, 200

proof, chloroform and anhydrous were purchased from Pharmaco. PLGA scaffolds were developed by Mirani [40].

2) PCL

For the purpose of generating Polycaprolactone (PCL) scaffold, Polycaprolactone of 47 kDa (Mw) was obtained from Polysciences (Warrington, PA). Type A porcine skin gelatin (approximately 300 bloom), low molecular weight Chitosan (50 kDa based on viscosity), Toluidine Blue O (with 90% dye content, approximately) and 500 kDa DS (contains 0.5-2.0% phosphate buffer salts) were purchased from Sigma Aldrich Chemical Co (St. Louis, MO). Glacial acetic acid was obtained from Pharmaco Products Inc (Brookfield, CN). Pure ethanol was purchased from AAPER (Shelbyville, KY). PLGA scaffolds were developed by Kornkorn [32]

4.1.2. Scaffold Formation

The PLGA composite scaffolds were prepared by 4 steps which is explained briefly [71]. Firstly, a thin PLGA film is formed by air drying PLGA solution (4 % 21 wt/v) which is prepared by dissolving the polymer pellets in 5mL chloroform stirred overnight. This is placed on a 8cm×6cm Teflon sheet (United States Plastic, Lima, OH) on which is a chemical fume hood fixed to a flat aluminum plate in order to form the thin film. The PLGA film that is formed as a result of air drying has a smooth and hydrophobic surface. Secondly, in order to perform the etching process the formed PLGA film was submerged completely in 1N NaOH solution for 10 minutes. This process helps

to create roughness elements on the surface of the film which is smooth and also makes the PLGA film hydrophilic. Thirdly, the etched PLGA film is washed with excess water and holes are punched on the surface in a square pitch which are 1 cm apart from each other using a hammer and stainless steel needle. Finally, the PLGA film is layered with a 3 mL mixture of 0.5 % (wt/v) gelatin and 0.5 % (wt/v) chitosan solution dissolved in 0.7% (v/v) acetic acid, on both the sides and is freeze dried in a lyophilizer in order to form the porous layer. Scanning Electron Microscope (SEM) was used to analyze the etching on the surface of the thin PLGA films.

For preparing PCL scaffolds, first, 3-4 mL of 10% (wt/v) PCL solution is prepared in glacial acetic acid. This solution was gently dropped on the surface of water in two inches diameter Teflon dish and was air dried until the matrix was completely formed. Neutralization of the matrix was done using ethanol for ten minutes. Neutralized matrix was then washed with water. “Top side” is the side that never touched water during formation and “bottom side” is the other side. In order to accomplish better comparison of PCL matrices formation, PCL matrices were formed by air drying 2 mL PCL solution (10% w/v) in chloroform

SIS also was utilized. SIS is a natural matrix rich in Type-1 collagen and the mechnical and physicochemical characteristics of the SIS matrix, such as thickness, permeability, ultrastructural properties and mechanical properties have been well characterized [1] and studied. SIS is a dense connective tissue which is obtained after removing the serosa, mucosa and muscle layers from the small intestine.

The PLGA and SIS scaffolds were prepared by Rahul Mirani while the PCL scaffolds were prepared by Kornkorn Makornkaewkeyoon.

4.1.3 Tensile Test

Initially, it is required to calculate the cross sectional area in order to perform the tensile tests. The thickness of the PLGA was measured using an inverted microscope [52, 71] by placing orthogonally wide strips of the composite matrix. Sigma Scan Pro (SYSTAT Software, Point Richmond, CA) software was used for measuring the thickness of the composite scaffolds. This measurement was conducted at various locations of the composite scaffold and an average value was used for tensile testing purposes. The same procedure was used to calculate the thickness of the PCL and SIS samples.

In order to do tensile testing, of freshly prepared samples, 5cm x 1cm rectangular strips were cut for PLGA and 12 mm x 30 mm rectangular strips were cut for PCL and were utilized for tensile testing in an INSTRON 5542 and INSTRON 5842 (INSTRON Inc., Canton, MA) mechanical testing machine respectively [56]. In brief, tests were performed at room temperature (25°C) for the dry condition and at 37°C for the wet condition (in phosphate-buffered saline (PBS) solution) [119]. The break stress and the corresponding strain were calculated using the software Merlin (INSTRON Canton, MA). Before performing the tensile test in the wet condition, for ten minutes the samples were incubated in 100% ethanol. The first and second elastic modulii of the scaffolds were calculated using the slopes of the portions that were linear in the stress-strain curve.

Tensile test on PLGA and SIS scaffolds were conducted by Rahul Mirani while the same on PCL scaffolds were conducted by Kornkorn Makornkaewkeyoon.

4.2 Ramp-and-Hold Test [32, 40]

In order to assess the viscoelastic properties of composite scaffolds, “Ramp-and-Hold” stress relaxation type experiments were performed. Tensile analysis performed prior to this helped in fixing the operating range so that the break strain is not reached while conducting the “Ramp-and-Hold” experiments. There were two major portions in the “Ramp-and-Hold” experiments. They were the loading portion and the relaxation portion. Loading portion is where a constant rate of tensile strain is enforced on to the composite scaffold sample for a particular predetermined amount of strain. In the relaxation portion of the experiment there is zero rate of loading, instead the composite scaffold sample is held at the strain value that was recorded at the end of the completion of the loading portion. The viscoelastic pseudo-component models were developed for the stress vs time experimental data that resulted from the “Ramp-and-Hold” test experiments. “Ramp-and-Hold” test experiments were conducted for 4 or 5 stages each of which had one loading and relaxation period.

Ramp-and-hold test on PLGA and SIS scaffolds were conducted by Rahul Mirani while the same on PCL scaffolds were conducted by Kornkorn Makornkaewkeyoon.

4.3 Optimization

Various optimization techniques Cyclic, RLM2 and Leapfrogging were used for determining the model parameters that best fit the experimental “Ramp-and-hold” data. The model parameters were adjusted by the optimizer so that the sum of squared deviations of the model from the experimental data for the entire range with 4 or 5 stages of sequential stretch-and-hold process is minimal.

The number of trials for which with 99% confidence the best-of-N random starts will result in one of the best 13% of all possible values for the SSD gives the N value as follows [30]

$$N = \frac{\ln(1-0.99)}{\ln(1-0.13)} = 34 \quad (4.1)$$

Hence 34 trials were required to determine the model parameters that best fit the experimental data.

The code for the optimization techniques was written in VBA. The initial guesses for each start was guessed as a set of random numbers that were generated randomly by the VBA code. The optimization techniques were conducted on PLGA, PCL and SIS samples to determine the model parameters that best fit the experimental data. For each of the scaffold samples each of the composite models developed were used to get the model parameters and the results were compared. The optimization techniques namely Cyclic, RLM2 and Leapfrogging conducted on the samples and the results were compared. In order to compare the optimization techniques in terms of their robustness, efficiency, time consumption and mathematical complexity along with number of function evaluations (NOFE) that were required to get the optimized parameters the optimization techniques were tested for different scaffold samples for different composite models and were compared with each other.

CHAPTER 5

RESULTS AND DISCUSSION

5.1 Model fitting for PLGA, PCL and SIS

The six composite 3 pseudo-component models developed were compared with the time-dependent experimental stress strain relationship as illustrated in Figure 5.1. Experimental tensile test data gave the stress-time relationship. From the data, the strain data was calculated using the strain rate. Strain increased in 4 or 5 stages, each with a ramp up in stress and then remained constant during which the material relaxed. Here it should be noted that for the same strain data, various experimental results were obtained i.e. due to experimental vagaries many experimental data sets gave higher or lower stress values. For each of the tissues one of the experimental data sets was considered for modeling as the representative one best characterizing the shape and magnitude of the stress response.

5.1.1 PLGA

PLGA stress time data was obtained [40]. The strain rate for PLGA is 3.125%. With the help of the optimizer, the fitting of the experimental data with the six different composite models was tested. With 99% confidence that the best-of-N random

starts will result in one of the best 13% of all possible values for the SSD gives the N value as 34 [30]. Observing the SSD, it was found that the composite Composite Model 4 did a better job compared to other models. Composite Model 4 is a combination of hyper-elastic spring with one retain component and a spring-and-dashpot component. Composite Model 4 gave a least SSD of 0.542 MPa^2. Figure 5.1 shows the fitting of Composite Model 4 data with the experimental data. The dotted curve represents the experimental stress data while the continuous curve on it represents the modeled stress data.

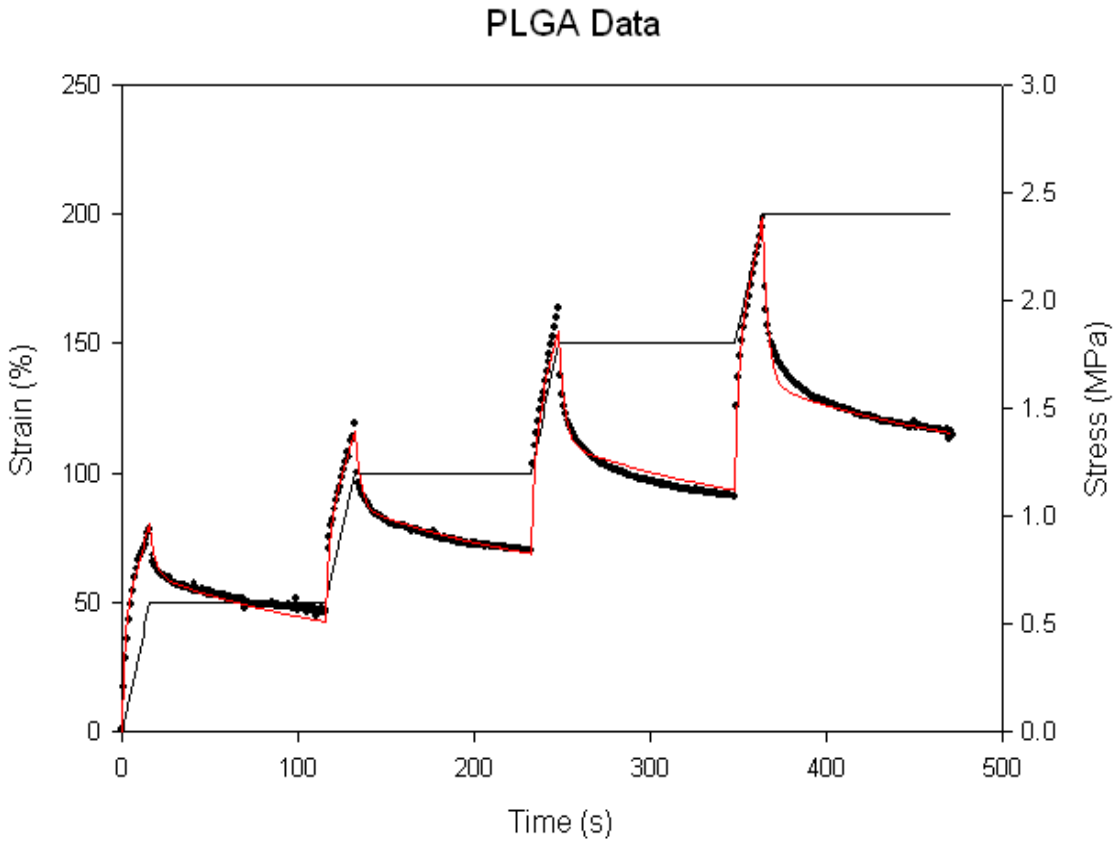

Figure 5.1: Experimental and Modeled stress vs. time for PLGA (Composite Model 4)

It can be seen in Figure 5.1 that the experimental data has a sharp rise in stress when the scaffold is strained and a rapid drop in stress with subsequent relaxation. Also, it can be seen that the rise in stress rise progressively increases with the same 50% strain increase. The experimental curve for the scaffold shows a good relaxation representation. Column 2 of Table 5.1 shows the lowest SSD values out of 34 trials for each of the different composite models along with their respective model parameter values that gave the least SSD.

Table 5.1: SSD and parameter values for various composite models for PLGA

Model	SSD (MPa^2)	ϕAx1 (MPa)	B1	ϕAx2 (MPa)	B2	Tau2(s)	ϕAx3 (MPa)	B3	Tau3(s)
1	1.77E+00	-1.37E+00	-9.90E-01	1.00E-02	4.49E+00	7.47E+01	-1.47E+00	-6.14E+00	2.77E+00
2	5.69E+00	1.29E+00	3.20E-01	2.28E+00	3.60E-01	2.40E+02	-7.70E-01	-1.64E+02	4.15E+00
3	1.12E+00	-1.52E+00	-8.10E-01	1.80E-01	1.04E+00	6.26E+01	1.95E+01	3.40E-01	1.58E+00
4	5.40E-01	-5.02E+00	-1.40E-01	-3.90E-01	-2.65E+01	1.20E+02	2.26E+00	7.90E-01	3.07E+00
5	2.01E+00	1.90E-01	8.60E-01	-3.67E+00	-2.11E+00	2.49E+00	-2.73E+00	-4.50E-01	4.81E+02
6	9.30E-01	-3.31E+00	-2.70E-01	1.35E+00	9.20E-01	3.96E+00	-4.90E-01	-1.60E+02	6.79E+01

A good approximation of the model data with the experimental data can be seen. In Figure 5.1 the dots represent the experimental stress time data. The solid line represents the generated strain time relationship. The continuous curve on the dots represents the fitting of the model data with the experimental data. It can be seen that the model data provides a close fit to the experimental data. The model as such captures large features like sharp rise in the stress value and immediate drop in stress values. Also, the model is able to capture the progressive increase in the stress value with the same 50% strain increase. Even then there are spots where the model does not capture the experimental behavior perfectly. Hence in general the model is good but not perfect as it does not provide an exact fit throughout. In this work, one model is used for all stages. One model

progressively fits all the stages. The number of model parameters, 8, which is fully adequate to Composite Model 4 successive strain-and-hold stages, is equivalent to the number needed for analytical models which could only model one strain and hold event.

5.1.2 PCL

PCL stress time data was obtained [32]. The strain rate for PCL is 1%. Like before the 6 composite models were tested for PCL data and the SSD was calculated for each of the composite model. It was found that composite Model 1 gave the lowest SSD of 0.395 MPa^2. Composite Model 1 is a combination of hyper-elastic spring with two spring-and-dashpot components. Fig 5.2 shows the fitting of Composite Model 1 data with the experimental data for PCL data.

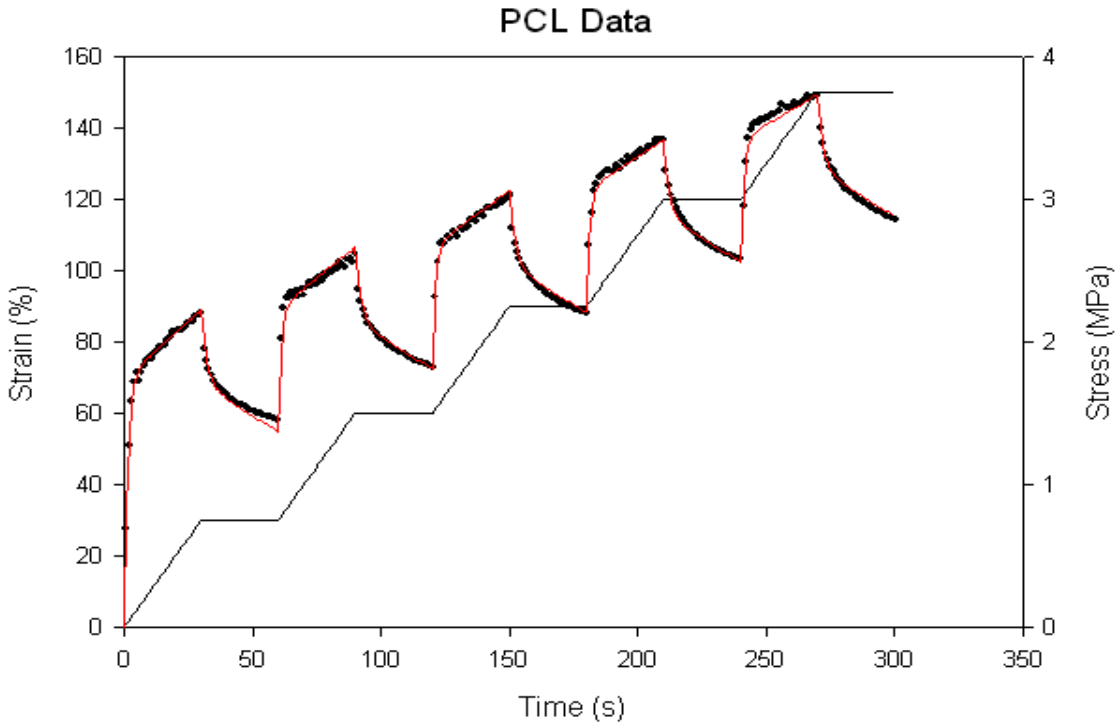

Figure 5.2: Experimental and Modeled stress vs. time for PCL (Composite Model 1)

Figure 5.2 shows that the experimental curve shows a large initial stress increase and then shows nearly identical stress increase for subsequent strain. Also the experimental data does not show sharp peaks like PLGA. The models developed are flexible enough to capture peaks for PLGA and flattened peaks for PCL. Model data gives a better fit to the experimental stress time data for PCL scaffold. Composite model 1 did the best job compared to all other models. F-Test done for 315 data points by extrapolating F-critical value for 20, 30, 40, 60 and 120 data points showed that statistically significantly Composite Model 1 is better than Composite Model 4 at 95 % confidence level. Table 5.2 shows the lowest SSD values out of 34 optimizer trials for each of the different composite models along with their respective model parameter values that gave the least SSD among the 34 optimizer trials.

Table 5.2: SSD and parameter values for various composite models for PCL

Model	SSD (MPa^2)	ϕAx1 (MPa)	B1	ϕAx2 (MPa)	B2	Tau2(s)	ϕAx3 (MPa)	B3	Tau3(s)
1	3.90E-01	-4.80E+00	-3.60E-01	-9.10E-01	-5.89E+01	2.06E+00	-1.25E+00	-6.31E+01	9.02E+01
2	3.79E+00	3.88E+00	2.90E-01	-1.35E+00	-5.62E+02	5.35E+00	-1.14E+00	-6.52E+00	6.10E+04
3	1.62E+00	-1.19E+00	-6.30E+01	1.69E+02	2.00E-01	1.71E+00	4.42E+00	3.20E-01	3.03E+02
4	4.90E-01	-4.94E+00	-3.50E-01	-1.30E+00	-7.96E+01	7.86E+01	-1.70E+03	-2.00E-02	1.39E+00
5	6.20E-01	-5.37E+00	-4.30E-01	-9.60E-01	-7.32E+01	5.23E+00	-8.80E-01	-6.93E+01	9.08E+06
6	8.10E-01	-4.20E+00	-6.40E-01	4.13E+01	5.00E-01	1.45E+00	-1.43E+00	-9.86E+01	5.26E+01

When the material is elongated there will be a reduction in the cross sectional area of the material. Hence when the PCL scaffold is repeatedly stretched and relaxed it should be noted that there will be a reduction in cross sectional area. But Composite Model 1 is a combination of hyper-elastic spring with two spring-and-dashpot components. These components do not account for the reduction in cross sectional area. The models having retain and reform component which account for the reduction in cross sectional area could

not do a better job than the one that did not account for the reduction in cross sectional area. Although there is a possibility for internal tearing of the tissue with stretching and reduction in cross sectional area, the Composite Model 1 is consistent with the experimental data obtained with stretching.

5.1.3 SIS

SIS stress time data was obtained [40]. The strain rate for SIS is 3.125%. The same kind of modeling that was done for PCL and PLGA was done for SIS data for 34 trials and the SSD was calculated for each of the models and was compared. Out of all the composite models tested, Composite Model 4, a combination of hyper-elastic spring with one retain component and a spring-and-dashpot component did the best job by giving a SSD value of 0.48 MPa^2. Figure 5.3 shows the fitting of the experimental data with the model data.

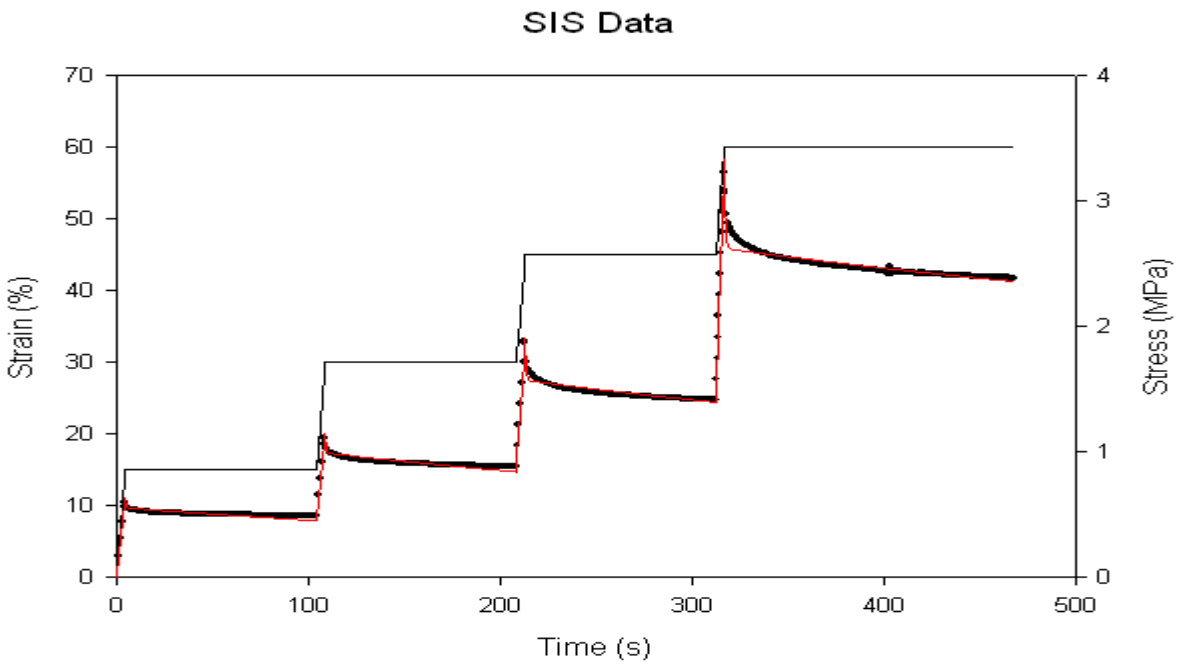

Figure 5.3: Experimental and Modeled stress vs. time for SIS (Composite Model 4)

Figure 5.3 shows that the experimental data shows sharp peaks similar to PLGA. The stress shows progressive increase from the previous value with subsequent strains. The experimental data also shows good relaxation representation. The model provides a good fit which is seen in Figure 5.3 but it is not perfect fit it is not providing an exact fit for the experimental stress in certain spots. But, as such, model stress time data obtained using Composite Model 4 and experimental stress time data are in close approximation. F-test showed that statistically significantly Composite Model 4 is better than Composite Model 6. For all the 4 stages of "Ramp-up-and-hold" the same model was used. Table 5.3 shows the SSD and parameter values for various composite models for the SIS data.

Table 5.3: SSD and parameter values for various composite models for SIS

Model	SSD (MPa^2)	ϕAx1 (MPa)	B1	ϕAx2 (MPa)	B2	Tau2(s)	ϕAx3 (MPa)	B3	Tau3(s)
1	1.77E+00	2.20E-01	3.91E+00	4.43E+00	2.58E+00	7.10E-01	-8.70E-01	-3.61E+00	2.51E+02
2	2.68E+00	4.00E-01	3.18E+00	3.94E+00	4.60E-01	1.44E+02	-3.90E-01	-1.60E+02	1.55E+00
3	6.70E-01	2.20E-01	4.00E+00	2.80E-01	4.69E+00	1.18E+00	-8.30E-01	-4.19E+00	3.09E+02
4	4.80E-01	9.80E-02	4.96E+00	-1.19E+00	-3.13E+00	3.79E+02	3.80E-01	5.05E+00	5.50E-01
5	1.69E+00	1.40E-01	4.51E+00	3.24E+02	4.00E-02	6.70E-01	-1.63E+00	-1.80E+00	3.94E+02
6	6.50E-01	2.70E-01	3.68E+00	1.90E-01	4.57E+00	2.08E+00	-5.80E-01	-6.29E+00	3.64E+02

For both PLGA and SIS scaffolds the pseudo component model with one retain component which accounts for the reduction in cross sectional area gives the best fit compared to others. In the case of PLGA and SIS the model that best fit the experimental data also explains the behavior of the real tissue.

5.2 Literature Data Validation

Transient stress relaxation data for Enzymatically Digested Bovine Annulus Fibrosus Tissue (EDBAFT) was obtained from Delphine. S. Perie, *et al* [120]. The composite models developed using the pseudo components were applied to this literature data. For validating the usage of these six composite models two criteria were tested. One of them being the sufficiency of models having eight parameters and other being that though there are nine parameters one of the pseudo component acts as a hyper-elastic spring because of one very high time constant value. Figure 5.4 shows the fitting of literature data with model data. Composite Model 4 did the best job compared to other models.

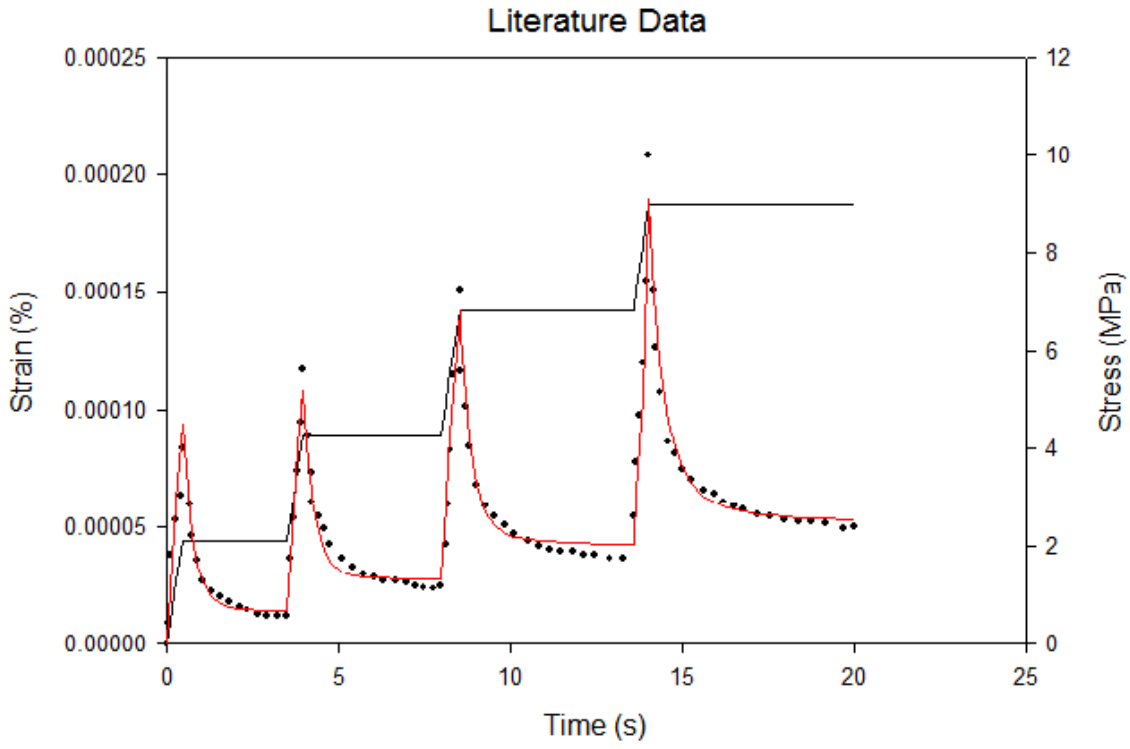

Figure 5.4: Fitting of the literature data using the pseudo-component model

Table 5.4 shows the various model parameter values for various composite models along with their respective SSD values.

Table 5.4: SSD and 8 parameter values for various composite models for EDBAFT

s

Model	SSD (MPa^2)	ϕAx1 (MPa)	B1	ϕAx2 (MPa)	B2	Tau2(s)	ϕAx3 (MPa)	B3	Tau3(s)
1	1.78E+01	-7.23E+01	3.00E-03	8.40E-01	1.25E+06	1.25E+01	1.06E+04	1.30E+03	4.00E-01
2	2.06E+01	4.10E-01	1.05E+06	5.41E+02	1.78E+03	6.75E+00	-8.27E+02	-1.75E+04	4.20E-01
3	1.05E+01	8.00E-02	1.73E+06	1.81E+01	4.84E+05	3.50E-01	1.07E+04	2.16E+02	5.30E+00
4	8.63E+00	4.13E+02	3.21E+03	-4.46E+02	-2.46E+04	5.60E-01	0.00E+00	3.92E+06	2.30E-01
5	2.07E+01	5.00E-01	9.77E+05	6.03E+01	1.26E+04	6.97E+00	7.00E+03	2.11E+03	4.30E-01
6	1.27E+01	-4.04E+02	-1.64E+03	1.83E+01	4.84E+05	4.60E-01	6.53E+02	1.10E+03	6.71E+07

It can be seen from the table that composite model 4 did a better job compared to other models. Composite Model 4 is a combination of a hyper-elastic spring with one retain component and a spring-and-dashpot component.

The modeling of the experimental data was also done with nine parameters (three pseudo-components, each of which had A, B and τ parameters). It was found that the least SSD value obtained was 8.33 MPa^2. On comparing this with the least value obtained by using 8 parameters it was seen that there was not a statistically significant difference between the SSD values when the number of parameters were increased.

Table 5.5 shows that the largest time constant values are very high for the composite models showing that one of the pseudo-components did not effectively relax.

Table 5.5: Largest time constant value for various composite models for EDBAFT

Model	Tau(s)
1	8.55E+04
2	6.71E+06
3	7.32E+04
4	1.06E+05
5	1.21E+06
6	6.52E+07

A non-relaxing element would be a hyper-elastic spring. This validates the usage of eight parameter models for modeling the soft tissues. Hence we use Architecture C.

5.3 Leapfrogging [31]

Leapfrogging as an optimizer was compared with two other optimizers namely the Rhinehart modified Levenberg Marquardt (RLM2) [117] optimizer and R^3 cyclic optimizer [117] for studying its efficiency and robustness. RLM2 algorithm is gradient based whereas both Leapfrogging and R^3 cyclic are direct search techniques. In order to compare the various optimizers the least SSD of the model data from the experimental data was used. Also, the number of function evaluations (NOFE) for each of the optimizers is compared. NOFE is the measure of work that each optimizer takes to calculate the model values. Finally, the probability of getting a particular objective function (OF) value (here it is the sum of square deviation of the experimental data from the model data) for various optimizers is compared. The RMS-RS [115-116] stopping criteria is used for all the techniques. Leapfrogging had 20 players while R^3 Cyclic had 1.05 as the expansion factor and 0.8 times the inverse of the expansion factor i.e. 0.76 as

the contraction factor. Table 5.6 lists the SSD and NOFE for various optimizers, from best of N (34) trials, for PLGA, PCL and SIS scaffold.

Table 5.6: SSD and average NOFE (ANOFE) values for various optimizers for PCL data

	Leapfrogging		RLM2		Cyclic	
	SSD (MPa^2)	ANOFE	SSD (MPa^2)	ANOFE	SSD (MPa^2)	ANOFE
PLGA	0.541	3,342	0.569	35,265	0.568	21,234
PCL	0.395	4,460	0.439	32,446	0.440	19,493
SIS	0.481	3,767	0.552	34,498	0.555	20,987

It can be observed from Table 5.6 that Leapfrogging as an optimizer gives the least SSD value compared to other optimizers, but there is not much of a difference between the SSD values that each of the optimization technique gave. The major difference is seen in the number of function evaluations (NOFE) each of the optimizer takes to calculate the best model parameter values. While Leapfrogging needs function evaluations of the order of 4,000, RLM2 and Cyclic require almost 10 times more and 5 times more respectively. This clearly shows that Leapfrogging is better in terms of computational effort than the other two optimizers.

Figure 5.5 shows the probability distribution function (PDF) of the OF for various optimizers vs the OF values. Each of the optimizer was run for 100 trials. The OF values obtained were arranged in ascending order and they were plotted again with the probability ranging from 0% to 100%. This procedure was done on PCL scaffold.

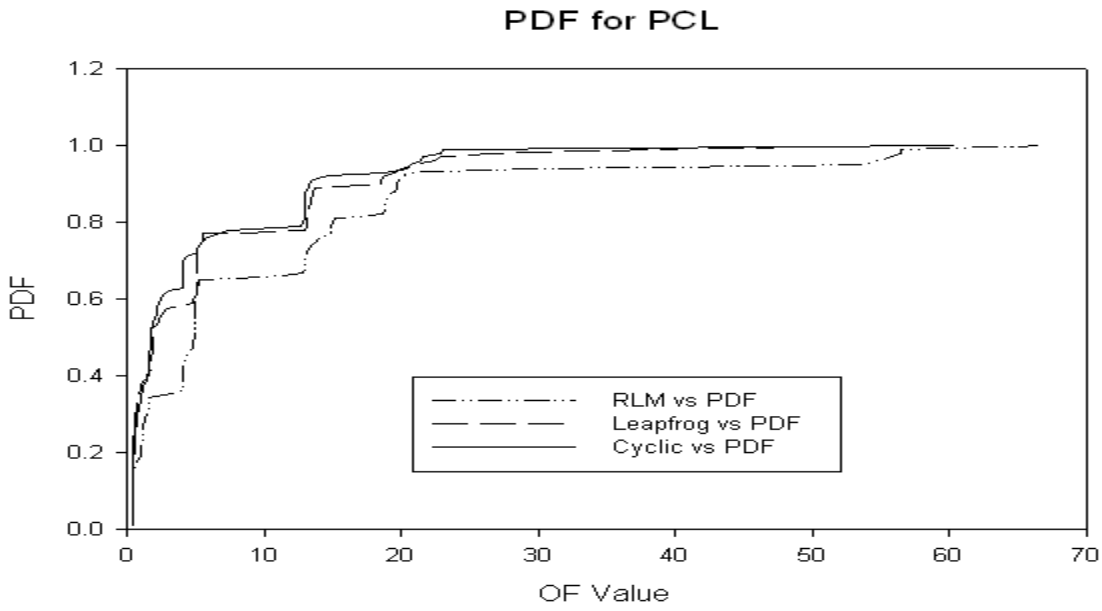

Figure 5.5: Probability density function for OF values using various optimizers on PCL data.

Table 5.7 lists the probability of achieving OF value for various optimizers on the PCL data. This table also includes the average NOFE for 100 trials.

Table 5.7: Probability of OF values and average NOFE values for various optimizers for PCL data

	OF values (Probability of attaining that value (%))					
	0.4	**4**	**15**	**20**	**35**	**NOFE**
Leapfrogging	2	58	90	94	100	4,220
Cyclic	1	64	92	94	100	19,783
RLM2	0	36	78	90	93	32,480

From Table 5.7 it can be seen that in comparison to Leapfrogging and Cyclic, RLM2 gives a lower probability for all the OF values. Hence, it can be clearly seen that Leapfrogging and Cyclic have a higher probability of finding its global optimum, than

RLM2. This shows that direct search techniques do a better job than gradient based techniques for this regression challenge. Though there is a difference in the probability for finding that OF using Leapfrogging and Cyclic it should also be noted that the Cyclic optimization technique needs almost more than 5 times the NOFE of what Leapfrogging requires. The probability of getting an OF value using Leapfrogging and Cyclic techniques are almost the same. The NOFE value for Leapfrogging makes it a better optimizer than Cyclic. Hence, Leapfrogging was best suited as an optimization technique than RLM2 and Cyclic optimization technique.

Leapfrogging as an optimization technique can be used with varying number of players. It is important to choose an optimized number of players in order to both minimize the computational burden and also to maximize the probability of reaching the global optimum value. Leapfrogging optimization technique was tested on PCL for various number of players. Table 5.8 presents the SSD value obtained for each of the different number of players along with the corresponding average NOFE.

Table 5.8: SSD and ANOFE values for various number of players

	Leapfrogging	
Number of players	SSD (MPa^2)	NOFE
10	0.405	4,034
20	0.395	4,220
50	0.394	4,657

From Table 5.8 it can be clearly seen that optimization technique with 50 players did the best job. But, it can also be seen that there is statistically no significant difference between the SSD values between 50 and 20 players. But, there is statistically significan difference between 10 players and 20 players. Also, the table shows that as the number of

players increases the NOFE value increases. Judgment for an optimal choice between the SSD and the NOFE values is the usage of 20 players. Hence, for this study Leapfrogging as an optimization technique with 20 players was used.

5.4 Model Extensions

The PLGA and SIS scaffold had four "ramp-up-and-hold" stages whereas PCL had five stages. The first three stages of the scaffold were modeled and the model parameters were used to project the model data to the rest of the stages.

PLGA:

Out of the four "ramp-up-and-hold" stages, three stages were modeled using various Composite Models. Using the model parameters that gave the least SSD value for the three stages, the model was projected forward for the last stage. Figure 5.6 shows the model projection of composite Model 4 from 3 stages to 4 stages for a PLGA scaffold.

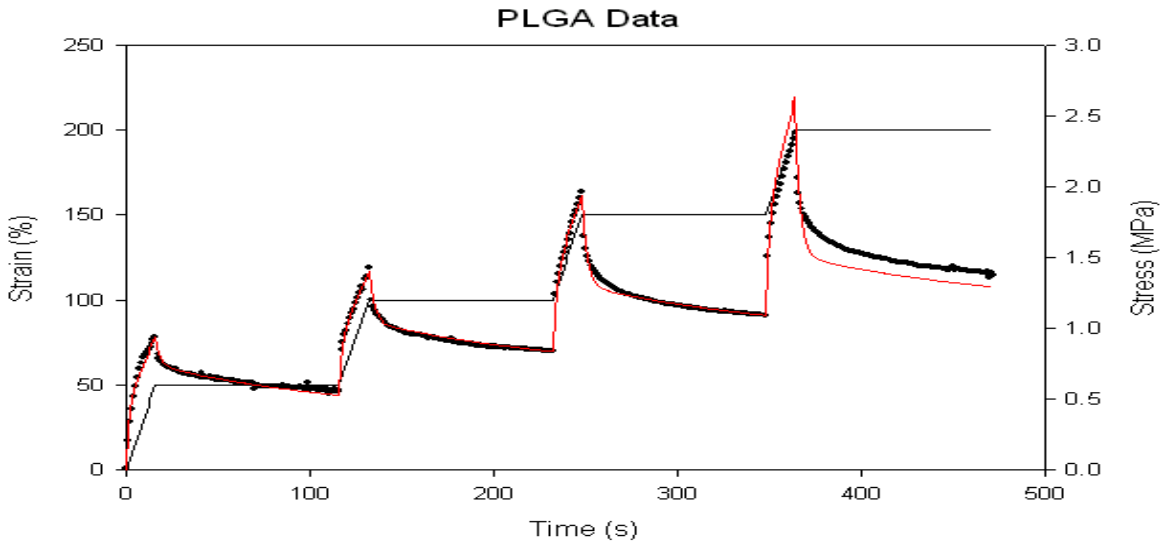

Figure 5.6: Experimental and Modeled stress vs. time for PLGA (Composite Model 4) with model projection from first three stages

Table 5.9 lists the overall SSD values obtained for all stages using the model parameters obtained for modeling the first 3 stages for various composite models along with the model parameters.

Table 5.9: SSD and parameter values for various composite models for PLGA

Model	SSD (MPa^2)	ϕAx1 (MPa)	B1	ϕAx2 (MPa)	B2	Tau2(s)	ϕAx3 (MPa)	B3	Tau3(s)
1	4.61E+00	-1.23E+00	-1.12E+00	4.30E-01	1.71E+01	9.30E-01	2.00E-02	4.77E+00	5.29E+01
2	1.05E+01	-2.06E+00	-3.20E-01	-6.40E-01	-1.64E+02	4.21E+00	5.20E-01	1.07E+00	2.07E+02
3	3.09E+00	-1.21E+00	-1.21E+00	1.90E-01	1.18E+00	4.11E+01	1.94E+01	4.10E-01	1.04E+00
4	2.33E+00	-2.17E+00	-3.80E-01	-3.60E-01	-2.91E+01	1.14E+02	1.33E+00	1.14E+00	2.66E+00
5	2.85E+00	-7.70E-01	-2.17E+00	1.20E+00	6.02E+00	1.42E+00	3.00E-02	3.60E+00	1.48E+02
6	4.21E+00	-2.05E+00	-5.00E-01	6.30E-01	1.44E+00	3.28E+00	-4.50E-01	-1.60E+02	7.08E+01

Again from Table 5.9 it can be seen that Composite Model 4 does the best job in comparison with other models in terms of SSD value. But, the SSD value obtained is greater than the SSD values that were obtained when all the stages were considered which is described in Section 5.1. Though the models developed fit the first three stages their projection is not so good when compared to direct fitting of all the stages which is evident from the high SSD value obtained as opposed to that obtained from Section 5.1. This is because of the complex behavior of the real tissue which the model is not able to capture. But, still the Model 4 does a better job which is evident from the SSD value obtained.

The same kind of modeling of first 3 stages and projecting it to the next 2 stages was done was done for the PCL scaffold. Since PCL scaffold had 5 stages the first 3 stages were modeled and the model parameters were projected to model the next 2 stages. Similar to modeling all stages in Section 5.1 Composite Model 1 did a better job than other models. But, still like in the case with PLGA the model projection did not capture all

the complexity of the tissue behavior. Figure 5.7 shows the model projection on all the stages.

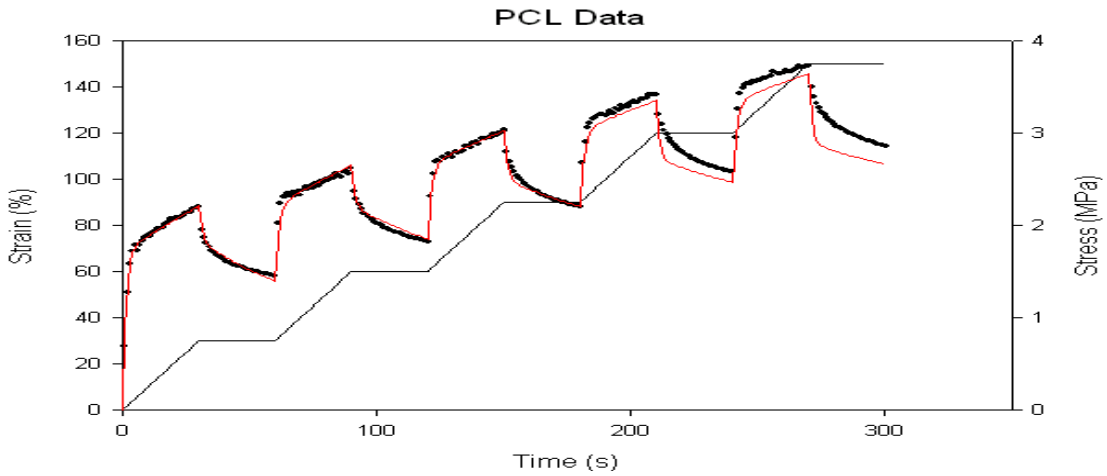

Figure 5.7: Experimental and Modeled stress vs. time for PCL (Composite Model 1) with model projection from first three stages

5.5 Multi Set Modeling

The code was modified to model multiple sets of experimental data in comparison to modeling of one set of data as was done before. The motivation was to capture experimental vagaries using the developed Composite Models. The experimental vagaries that were obtained in the data sets for each of the tissue was put together and was tried to be modeled using the Composite Models. Figure 5.8 shows modeling multiple sets of experimental data at the same time by using the Composite Model 1.

From Figure 5.8 it can be seen that though there were 2 sets of data for the same strain data, the model separately captured each of the experimental data but the fitting of the data was not so good which can be seen with the SSD value. Figure 5.8 shows the fitting of pseudo component model with two sets of data.

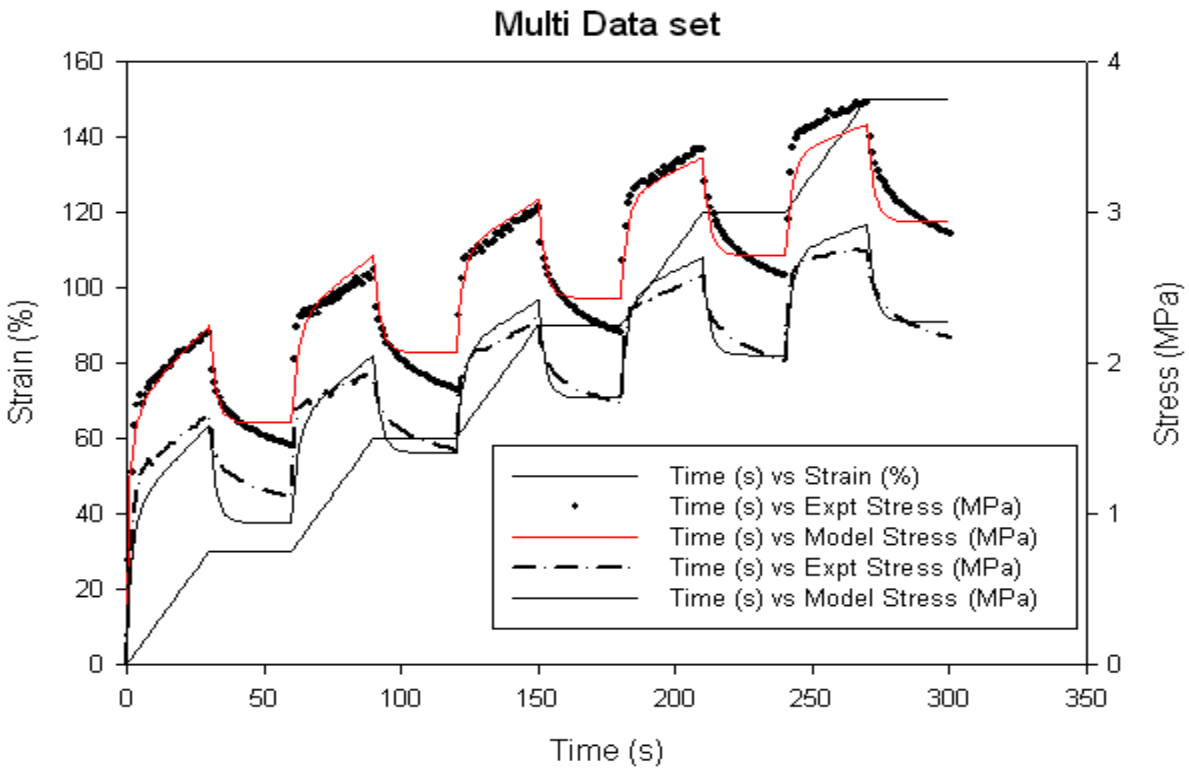

Figure 5.8: Experimental and Modeled stress vs. time for two data sets

The same pseudo component modeling was applied to 5 data sets vagaries and it was found that the model did not capture the experimental data separately. The model could not individually fit the experimental data. It should be noted that the strain data for both the sets of data was nominally the same. This shows that the models developed when used to model multiple sets of data simultaneously at the same time were are not able to capture individual sets of data and give suitable model data that best matches the experimental data. Figure 5.9 shows the fitting of model data with experimental data for 5 data sets.

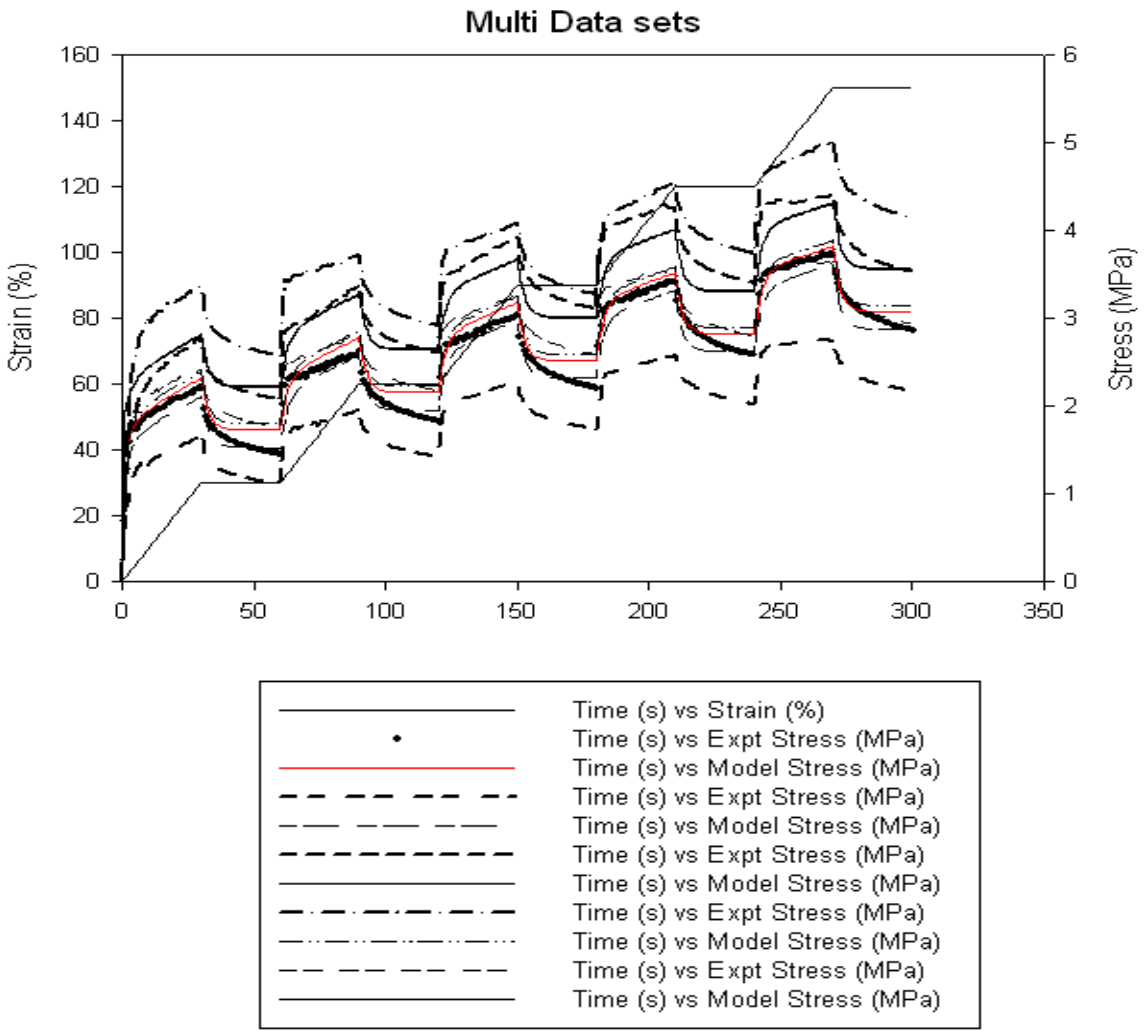

Figure 5.9: Experimental and Modeled stress vs. time for five data sets

It is important to know that all these data sets have the same nominal strain rate and same strain data. The same modeling of multi data sets was done with data sets with different strain rates. But different models could not be obtained that could better fit the data separately. It can be clearly seen from the Figure 5.9 that models for the first two data sets almost merged with each other. Similar is the case with the models for data sets 3 and 4 though there is clear variation between the experimental data sets.

5.6 Sensitivity

The model could not give a better fit to the experimental data when multiple data sets were used. Hence the sensitivity of the model to slight variations in time was tested. The time instance at which the experimental stress data was recorded was slightly changed. For this changed time instance the new strain data was calculated. Only few time instances out of the entire range were varied. The pseudo component models were applied to the new set of data using Leapfrogging as an optimization technique. It was found that the model did not show any visible sensitivity to changes in time instance.

The sensitivity of each of the model parameters towards giving a best fit to experimental data was tested. Table 5.10 lists the sensitivity of each of the parameter for PLGA, PCL and SIS.

Table 5.10: Sensitivity of each of the parameter on the SSD for each material

	Sensitivity							
	Ax1	Bx1	Ax2	Bx2	Tau2	Ax3	Bx3	Tau3
PLGA	5.00E-02	2.77E+01	4.00E-01	0.00E+00	0.00E+00	8.00E-01	4.15E-01	1.00E-01
PCL	4.63E+00	5.30E+00	8.50E-02	3.00E-02	5.00E-02	4.00E-01	3.50E-02	3.50E-02
SIS	7.50E-01	6.39E+01	2.82E+01	9.50E-01	0.00E+00	5.00E-02	3.00E-02	5.00E-02

It is seen from Table 5.10 that the sensitivity of the elastic power constant of the hyper-elastic spring was the highest among all the parameters. A small change in the elastic power constant value caused a drastic change in the SSD of the model data from the experimental data.

5.7 Cycling

A useful model will be able to translate to other stress-strain situations. As a demonstration of the transferability of this model, Figure 5.10 shows the model response for a cyclic strain application. Strain is steadily increased until stress reaches an upper limit, decreased at the same rate until stress reduces to a lower limit, and subsequently repeated. Figure 5.10 shows the cycling data for the PLGA model Architecture C, Composite Model 4.

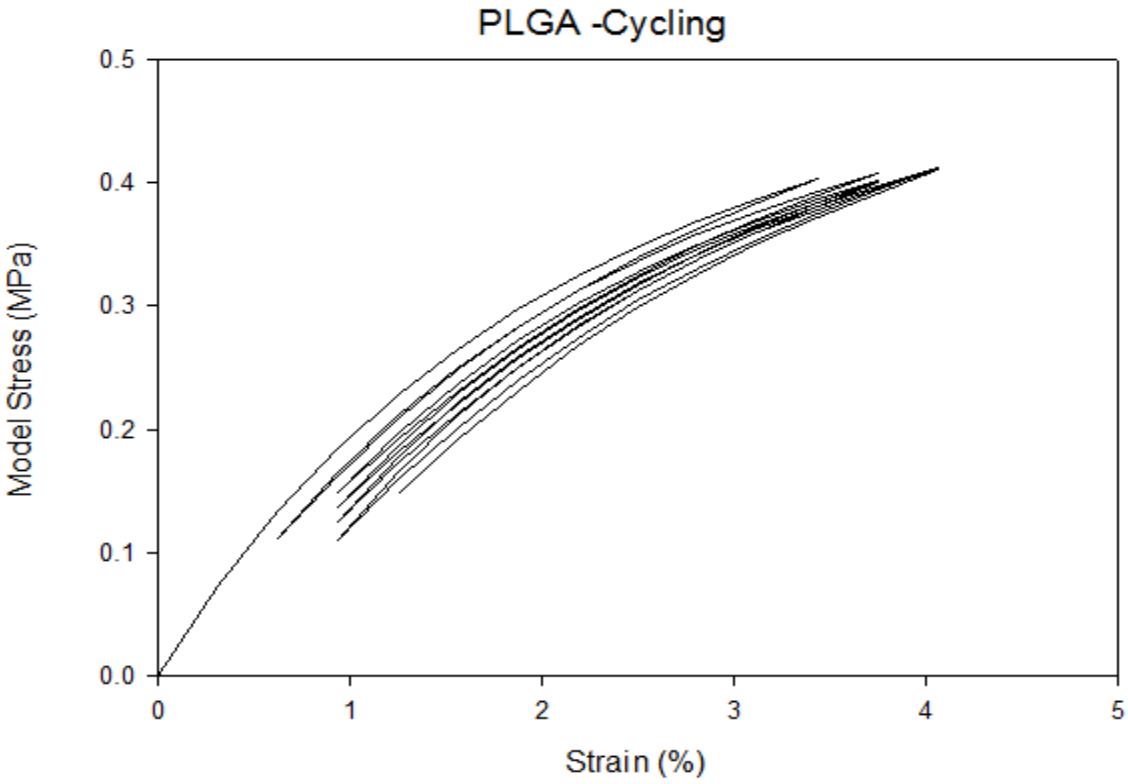

Figure 5.10: Cycling curve for PLGA Model 4.

The upper limit for the modeled stress was kept as 0.40 MPa whereas the lower limit was at 0.13 MPa for PLGA scaffold. Figure 5.10 shows that the strain progressively increases with each cycle, indicating that one of the components is reforming to the new

conditions. However, note that the strain increase between two consecutive cycles progressively decreases. Eventually, not shown, subsequent cycles overlap each other. PLGA is an amorphous material. Figure 5.10 reveals that it does not "give" or "yield" much when strained. Continuous stretching and relaxing should as such keep cycling over the same cycle again and again. This behavior is similar to what would happen experimentally, further revealing transferability of the models to other situations.

The same demonstration of transferability of the model that fit the experimental data was tested for PCL and SIS data. Figure 5.11 and Figure 5.12 show the cycling nature of the Composite Model 1 and Composite Model 4 for PCL and SIS respectively.

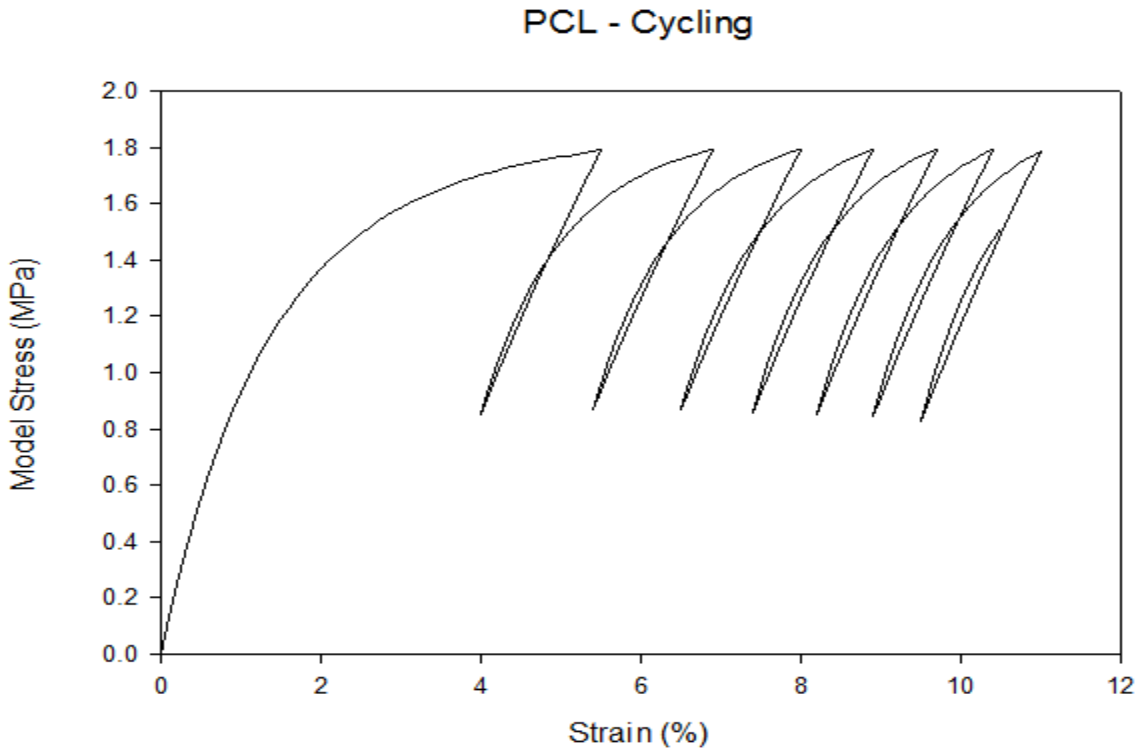

Figure 5.11: Cycling curve for PCL Model 1.

The limits were 1.8MPa and 0.8MPa for the PCL data. Transferability of Composite Model 4 for the SIS data could be better seen for the PCL data with the cycles

overlapping each other. PCL is semi-crystalline. Figure 5.11 reveals that PCL "gives" or "yields" when each strain stage is greater than about 5%. So repeated stretching and relaxing should keep expanding the material and it should not cycle again and again which is the same that is illustrated by the Composite Model 4. Stress gets accumulated progressively with successive application and removal of strain which is what is expected happen explaining transferability of the model.

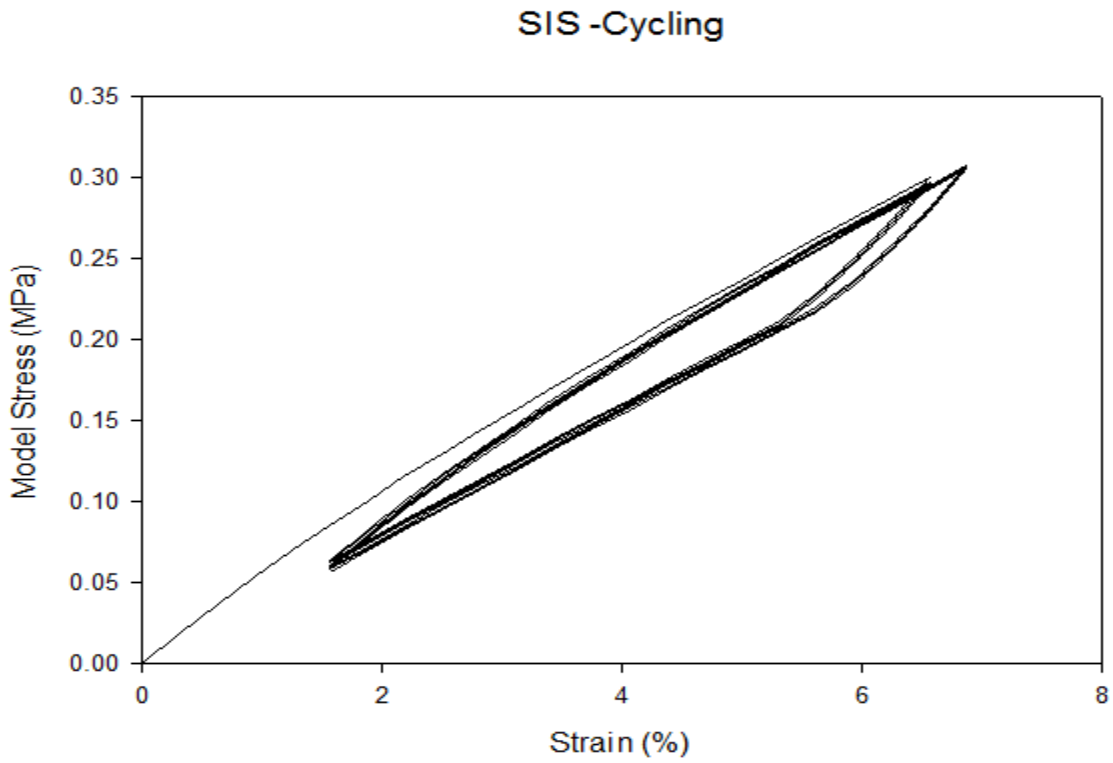

Figure 5.12: Cycling curve for SIS Model 4.

The upper and lower limits were respectively 0.30 MPa and 0.063 MPa for the SIS data. Here Figure 5.12 shows that the cycles overlap with each other as required and expected showing the transferability of the Composite Model 4. SIS is a perfect viscoelastic material. Repeated stretching and relaxing should make it cycle over the same

region again and again because as such there would be no stretching of the material which clearly explains the hysteresis of the viscoelastic material. This is very well seen from the behavior of the Composite Model which suggests that the Composite Model well captures the behavior of the tissue.

CHAPTER 6

CONCLUSIONS AND RECOMMENDATIONS

6.1 Conclusion

In order to accomplish the objective the following research was conducted:

1) Six constitutive models were developed using combinations of any three of the four viscoelastic components namely hyper-elastic spring, spring-and-dashpot, reform and retain in parallel to model complex tissue structures.

2) Various optimization techniques such as RLM2, Cyclic and Leapfrogging were tested for their efficiency and robustness in obtaining best set of model parameters. It was found that Leapfrogging did the best job in comparison with other optimizers and hence Leapfrogging was considered as the optimization technique for this study because of its robustness and effectiveness in finding the OF with lesser number of function evaluations.

3) Testing of the six Composite Models on PLGA, PCL and SIS tissue scaffolds showed that Composite Model 4 which is a combination of a hyper-elastic spring

with one retain and a spring-and-dashpot component modeled PLGA and SIS very well compared to other Composite Models. It was also found that Composite Model 1 best modeled PCL tissue scaffold.

4) The sufficiency of the developed Composite Models having eight model parameters was tested and it was found that eight model parameters are enough to best model the complex tissue structures.

5) The developed Composite Models were successfully tested on literature data.

6) The Composite Models were tested for their efficiency in modeling first 2 or 3 ramp-up-and-hold stages and hence project itself through other stages. They did not prove to be very efficient in terms of returning a better sum of square deviation value than what was returned by modeling all stages together.

7) The Composite Models were used to model the experimental vagaries that was obtained for the same strain data. But they could not model the experimental vagaries. The models could match for stress vs time data for any sample, but there was little sample-to-sample consistency to say that model parameters represent the truth about the material.

8) The six Composite Models were tested for their sensitivity and it was found that they were not sensitive to very small changes in the time data.

9) In order to accept the developed Composite Models, the Models were checked for their transferability, meaning that when model parameter values were obtained from sequential ramp-up-and-hold data, the parameterized models would generate cyclic stress-strain data which qualitatively matches the expectation. It was observed that the Composite Models demonstrated transferability for the tissues PLGA, PCL and SIS.

10) The six Composite Models along with the optimization techniques were written as a code in MS Excel/ VBA which could be made available for convenient access.

6.2 Future Work

Recommendations for future work are:

1) Modify the model in such a way that it can account for the experimental vagaries that are obtained as a result of experiments conducted.

2) Modify the model to model few stages of "Ramp-up-and-hold" and hence project the future behavior of the tissue which would help in knowing how a real complex tissue would behave in future. Look at alternate pseudo-component models (fluid rearrangement). Re-consider "best" models by goodness of projecting.

3) Generate experimental time-cyclic stress-strain behavior and see if 1) it can be used to generate models which reveal expected stress-time data for sequential ramp-up-and-hold conditions and 2) how well models developed from one test condition match behavior in the other.

4) Test the model on compression results.

5) Improve uniformity of experimental data (of experimental films) so that models can be more critically tested for transferability to new conditions and model parameter values can be correlated to fundamental material properties (molecular weight, etc)

6) Test under conditions that simplify the one-dimensional strain, perhaps on a larger sample.

7) Create models that account for two-dimensional orientation and internal shear.

8) Device pseudo-components which include internal tearing and elongation of voids.

REFERENCES

1. Rhinehart, RR, Madihally, SV, *Pseudo-Component Viscolelastic Model of Soft Tissues.* PD 04-1144 Biomolecular Systems Cluster Proposal.

2. Haslach Jr, HW, *Nonlinear Viscoleastic, Thermodynamically Consistent, Models for Biological Soft Tissue.* Biomech Model Mechanobiol, 2005. 3(3): p. 172-189.

3. Fung, YC, *Elasticity of Soft Tissues in Simple Elongation.* Am J Physiol, 1967. 213(6): p. 1532-1544.

4. Nekouzadeh, A, Pryse, KM, Elson, EL, Genin, GM, *A Simplified Approach to Quasi-linear Viscoelastic Modeling.* J Biomech, 2007. 40(14): p. 3070-8.

5. Duling, RR, Dupaix, RB, Katsube, N, Lannutti, J, *Mechanical Characterization of Electrospun Polycaprolactone (PCL): A Potential Scaffold for Tissue Engineering.* J Biomech Eng, 2008. 130(1): p. 011006.

6. Sarver, JJ, Robinson, PS, Elliott, DM, *Methods for Quasi-linear Viscoelastic Modeling of Soft Tissue: Application to Incremental Stress-relaxation Experiments.* J Biomech Eng, 2003. 125(5): p. 754-8.

7. Craiem, D, Rojo, FJ, Atienza, JM, Armentano, RL, Guinea, GV, *Fractional-order Viscoelasticity Applied to Describe Uniaxial Stress Relaxation of Human Arteries.* Phys Med Biol, 2008. 53(17): p. 4543-54.

8. Boyce, BL, Jones ,RE, Nguyen, TD, Grazier, JM, *Stress-controlled Viscoelastic Tensile Response of Bovine Cornea.* J Biomech, 2007. 40(11): p. 2367-76.

9. Defrate, LE, Li, G, *The Prediction of Stress-relaxation of Ligaments and Tendons Using the Quasi-linear Viscoelastic Model.* Biomech Model Mechanobiol, 2007. 6(4): p. 245-51.

10. Grashow, JS, Yoganathan AP, Sacks MS, *Biaxial Stress-stretch Behavior of the Mitral Valve Anterior Leaflet at Physiologic Strain Rates.* Ann Biomed Eng, 2006. 34(2): p. 315-325.

11. Holzapfel, GA, Eberlein, R, Wriggers, P, Weizacker, HW, *Large Strain Analysis of Soft Biological Membranes:Formulation and Finite Element Analysis.* Computer Methods in Applied Mechanics and Engineering, 1996. 132(1-2): p. 45-61

12. Jacob, X, Catheline, S, Gennisson, JL, Barriere, C, Royer, D, Fink, M, *Nonlinear Shear Wave Interaction in Soft Solids.* J Acoust Soc Am, 2007. 122(4): p. 1917-1926.

13. Weiss, JA, Gardiner, JC, Bonifasi-List, C, *Ligament Material Behavior is Nonlinear, Viscoelastic and Rate-independent Under Shear Loading.* J Biomech, 2002. 35(7): p. 943-950.

14. Lanir, Y, *Constitutive Equations for Fibrous Connective Tissues.* J Biomech, 1983. 16(1): p. 1-12.

15. Fung, YC, *Biomechanics: Mechanical Properties of Living Tissues*. 1982.

16. Olberding, JE, Francis Suh, JK, *A Dual Optimization Method for the Material Parameter Identification of a Biphasic Poroviscoleastic Hydrogel: Potential Application to Hypercompliant Soft Tissues.* J Biomech, 2006. 39(13): p. 2468-2475.

17. Picton, DC, Wills, DJ, *Viscoelastic Properties of the Periodontal Ligament and Mucous Membrane.* J Prosthet Dent, 1978. 40(3): p. 263-272.

18. Doehring, T, Einstein D, Freed, A, Pindera, M-J, Saleeb, A, Vesely, I, *New Approaches to Computational Modeling of the Cardiac Valves.* Anaheim, CA, United States: Acta Press, 2004: p. 134-137.

19. Abramowitch, SD, Woo, SL, *An Improved Method to Analyze the Stress Relaxation of Ligaments Following a Finite Ramp Time Based on the Quasi-linear Viscoelastic Theory.* J Biomech Eng, 2004. 126(1): p. 92-7.

20. Abramowitch, SD, Woo, SL, Clineff, TD, Debski, RE,*An Evaluation of the Quasi-linear Viscoelastic Properties of the Healing Medial Collateral Ligament in a Goat Model.* Ann Biomed Eng, 2004. 32(3): p. 329-335.

21. Funk, JR, Hall, G, Crandall JR, Pilkey WD, *Linear and Quasi-linear Viscoleastic Characterization of Ankle Ligaments.* J Biomech Eng, 2000. 122(1): p. 15-22.

22. Toms, S.R., Dakin, GJ, Lemons, JE, Eberhardt, AW, *Quasi-linear Viscoelastic Behavior of the Human Periodontal Ligament.* J Biomech, 2002. 35(10): p. 1411-5.

23. Woo, SL, Gomez, MA, Akeson, WH, *The Time and History-dependent Viscoelastic Properties of the Canine Medical Collateral Ligament.* J Biomech Eng, 1981. 103(4): p. 293-8.

24. Woo, SL, Peterson, RH, Ohland, KJ, Sites, TJ, Danto MI, *The Effect of Strain Rate on the Properties of the Medical Collateral Ligament in Skeletally Immature*

and Mature Rabbits: A Biomechanical and Histological Study. J Orthop Res, 1990. 8(5): p. 712-721.

25. Wineman, A, *Nonlinear Viscoelastic Solids--A Review*. Mathematics and Mechanics of Solids, 2009. 14(3): p. 300-366.

26. Zhong, C, *A Nonlinear Viscoelastic Model for Describing the Deformation Behavior of Braided Fiber Seals.* Textile Research Journal, 1995. 65(8): p. 461-470.

27. Provenzano, P, Lakes, R, Keenan, T, Vanderby Jr, R, *Nonlinear Ligament Viscoelasticity.* Ann Biomed Eng, 2001. 29(10): p. 908-14.

28. Marklund, E., Eitzenberger, J, Varna, J, *Nonlinear Viscoelastic Viscoplastic Material Model Including Stiffness Degradation for Hemp/lignin Composites.* Composites Science and Technology, 2008. 68(9): p. 2156-2162.

29. Hongbin, L., Noonan, DP, Zweiri, YH, Althoefer, KA, Seneviratne, LD, *The Development of Nonlinear Viscoelastic Model for the Application of Soft Tissue Identification.*

30. Iyer, MS, Rhinehart, RR, *A Method to Determine the Required Number of Neural Network Training Repetitions.* IEEE Transactions on Neural Networks, 1999. 10(2): p. 427-432.

31. Rhinehart, RR, Su, M, Manimegalai Sridhar, U, *Leapfrogging: A Novel Optimization Approach*, submitted to *European Journal of Optimizations Research*. 2010.

32. Makornkaewkeyoon, K, *Polycaprolactone Matrices Generated in Aqueous Media: Natural Polymers Immobilization and Stress Relaxation Behavior*, in *Chemical Engineering*. 2010, Oklahoma State University: Stillwater. p. 64.

33. Langer, R, Vacanti, JP, *Tissue Engineering.* Science, 1993. 260(5110): p. 920-926.

34. Woodruff, MFA, Nolan, B, Robson, JS, Macdonald, MK, *Renal Transplantation in Man : Experience in 35 Cases.* The Lancet, 1969. 293(7584): p. 6-12.

35. Schulak, JA, Bohnengal, A, Hanto, DW, Henderson, JM, Henry, ML, Walsh, TE, Ryckman, FC, *The Ohio Solid Organ Transplantation Consortium: A 15-year Experience.* Transplantation Reviwes, July 1999. 13(3): p. 135-147.

36. *United Network Organ Sharing Statistics*. 2009; Available from: http://www.unos.org/Resources/bioethics.

37. Bradbury, ET, Simons, W, Sanders, R, *Psychological and Social Factors in Reconstructive Surgery for Hemi-facial Palsy.* Journal of Plastic, Reconstructive & Aesthetic Surgery, March 2006. 59(3): p. 272-278.

38. Yuen, JC, Zhou, AT, Serafin, D,Georgiade, GS, *Long-term Sequelae Following Median Strenotomy Wound Inflection and Flap Reconsturction.* Ann Plast Surg, 1995. 35(6): p. 585-9.

39. Fishman, JA, Issa, NC, *Infection in Organ Transplantation: Risk Factors and Evolving Patterns of Infection.* Infectious Disease Clinics of North America, June 2010. 24(2): p. 273-283.

40. Mirani, R, *Stress Relaxation Modeling of Composite Porous Scaffolds*, in *Chemical Engineering*. 2009, Oklahoma State University: Stillwater. p. 85.

41. Oberpenning, F, Meng, J., Yoo, JJ, Atala, A, *DE Novo Reconstitution of a Functional Mammalian Urinary Bladder by Tissue Engineering.* Nat Biotechnol, 1999. 17(2): p. 149-155.

42. Chvapil, M, *Collagen Sponge: Theory and Practise of Medical Applications.* Journal of Biomedical Materials Research, 1977. 11(5): p. 721-741.

43. Langer, R, Vacanti, JP, Atala, A, Freed, LE, Vunjak-Novakovic, G, *Tissue Engineering : Biomedical Applications.* Tissue Engineering, 2007. 1(2): p. 151-161.

44. Khor, E, Lim, LY, *Implantable Applications of Chitin and Chitosan.* Biomaterials, 2003. 24(13): p. 2339-49.

45. Cheng, M, Deng, J, Yang, F, Gong, Y, Zhao, N, Zhang, X, *Study on Physical Properties and Nerve Cell Affinity of Composite Films from Chitosan and Gelatin Solutions.* Biomaterials, 2003. 24(17): p. 2871-80.

46. Hu, SG, Jou, CH, Yang, MC, *Protein Adsorption, Fibroblast Activity and Antibacterial Properties of Poly(3-hydroxybutyric acid-co-3-hydroxyvaleric acid) Grafted with Chitosan and Chitooligosaccharide After Immobilized with Hyaluronic Acid.* Biomaterials, 2003. 24(16): p. 2685-93.

47. Mao, J, Zhao, L, Yao, K, Shang, Q, Yang, G, Cao, Y, *Study of Novel Chitosan-Gelatin Artificial Skin In Vitro.* J Biomed Mater Res A, 2003. 64(2): p. 301-8.

48. Xia, W, Liu, W, Cui, L, Liu, Y, Zhong, W, Liu, D,Wu, J,Chua, K,Cao, Y, *Tissue Engineering of Cartilage with the Use of Chitosan-gelatin Complex Scaffolds.* J Biomed Mater Res B Appl biomater, 2004. 71(2): p. 373-380.

49. Harrison, JH, *Dextran as a Plasma Substitute with Plasma Volume and Excretion*

Studies on Control Patients. Ann Surg, 1954. 139(2): p. 137-42.

50. Jonga, SJ, De Smedtc, SC, Demeesterc, J, Nostruma, CF, Kettenes-van den Boschb, JJ, Henninka, WE, *Biodegradable Hydrogels Based on Stereocomplex Formation Between Lactic Acid Oligomers Grafted to Dextran.* J Control Release, 2001. 72(1-3): p. 47-56.

51. Hennink, WE, De Jonga, SJ, Bosa, GW, Veldhuisa, TFJ, van Nostruma, CF, *Biodegradable Dextran Hydrogels Crosslinked by Stereocomplex Formation for the Controlled Release of Pharmaceutical Proteins.* Int J Pharm, 2004. 277(1-2): p. 99-104.

52. Raghavan, D, Kropp, .BP, Lin, HK, Zhang, Y, Cowan, R, Madihally, SV, *Physical Characteristics of Small Intestinal Submucosa Scaffolds are Location-Dependent.* J Biomed Mater Res A, 2005. 73(1): p. 90-96.

53. Madihally, SV, Matthew, HWT, *Porous Chitosan Scaffolds for Tissue Engineering.* Biomaterials, 1999. 20(12): p. 1133-1142.

54. Zielinski, BA, Aebischer, P, *Chitosan as a Matrix for Mammalian Cell Encapsulation.* Biomaterials, 1994. 15(13): p. 1049-56.

55. Kang, HW, Tabata, Y, Ikada, Y, *Fabrication of Porous Gelatin Scaffolds for tissue Engineering.* Biomaterials, 1999. 20(14): p. 1339-44.

56. Sarasam, A, Madihally, SV, *Characterization of Chitosan-Polycaprolactone Blends for Tissue Engineering Applications.* Biomaterials, 2005. 26(27): p. 5500-5508.

57. Ayyildiz, A, Akgul, KT, Huri, E, Nuhoglu, B, Kilicoglu, B, Ustun, H, *Use of Porcine Small Iintestinal Submucosa in Bladder Augmentation in Rabbit: long-term histological outcome.* ANZ J Surg, 2008. 78(1-2): p. 82-86.

58. Oelschlager, BK, Pellegrini, CA, Hunter, J, Soper, N, Brunt, M, Sheppard, B, *Biologic Prosthesis Reduces After Laproscopic Paraesophageal Hernia Repair: a Multicenter, Prospective, Randomized Trial.* Ann Surg, 2006. 244(4): p. 481-490.

59. Petter-Punchner, AH, Fortelny, RH, Mittermayr, R, Walder, N, Ohlinger, W, Redl, H, *Adverse Effects of Porcine Small Intestine Submucosa Implants in Experimental Ventral Hernia Repair.* Surg Endosc, 2006. 20(6): p. 942-946.

60. Mostow, EN, Haraway, GD, Dalsing, M, Hodde, JP, Kind, D, *Effectiveness of an Extracellular Matrix Graft (OASIS Wound Matrix) in the Treatment of Chronic Leg Ulcers: a Randomized Clinical Trial.* J Vasc Surg, 2005. 41(5): p. 837-843.

61. Rose, PJ, Mark, HF, Bikales, NM, Overberger, CG, Menges, G, Kroschwitz, JI, in

Encyclopedia of Polymer Science and Engineering, M.H. Rose PJ, Bikales NM, Overberger CG, Menges G, Kroschwitz JI, Editor. 1989, Wiley: New York, USA.

62. Dubruel, P, Unger, R, Vlierberghe, SV, Cnudde, V, Jacobs, PJS, Schacht, E, KIrkpatrick, CJ, *Porous Gelatin Hydrogels : 2. In Vitro Cell Interaction Study.* Biomacromolecules, 2007. 8(2): p. 338-44.

63. Yin, Y, Fen, Y, Cui, J, Zhang, F, Li, X, Yao, K, *Preparation and Characterization of Macroporous Chitosan–Gelatin/β-tricalcium Phosphate Composite Scaffolds for Bone Tissue Engineering.* J Biomed Mater Res A, 2003. 67(3): p. 844-55.

64. Kim, BS, Mooney, DJ, *Development of Biocompatible Synthetic Extracellular Matrices for Tissue Engineering.* Trens Biotechnol, 1998. 16(5): p. 224-30.

65. Silva, EA, Mooney, DJ, *Synthetic Extracellular Matrices for Tissue Engineering and Regeneration.* Curr Top Dev Biol, 2004. 64: p. 181-205.

66. Tillman, J, Ullm, A, Madihally, SV, *Three-dimentional Cell Colonization in a Sulfate Rich Environment.* Biomaterials, 2006. 27(32): p. 5618-5626.

67. Langer, R, Tirrell, DA, *Designing Materials for Biology and Medicine.* Nature, 2004. 428(6982): p. 487-492.

68. Lelkes, PI, Mengyan, L, Perets, A, Mondrinos, MJ, Guo, Y, Chen, X, MacDiarmid, AG, Ko, FK, Finck, CM, Wei, Y, *Designing Intelligent Polymeric Scaffolds for Tissue Engineering: Blending and Co-electrospinning Synthetic and Natural Polymers.* Experimental Analysis of Nano and Engineering Materials and Structures, 2007: p. 831-832.

69. Chen, G, Sato, T, Ushida, T, Ochiai, N, Tateishi, T, *Tissue Engineering of Cartilage Using a Hybrid Scaffold of Synthetic Polymer and Collagen.* Tissue Engineering, 2004. 10(3-4): p. 323-330.

70. Lin, HB, Sun, W, Mosher, DF, García-Echeverría, C, Schaufelberger, K, Lelkes, PI, Cooper, SL, *Synthesis, Surface, and Cell-adhesion Properties of Polyurethanes Containing Covalently Grafted RGD-peptides.* J Biomed Mater Res 1994. 28(3): p. 329-42.

71. Lawrence, BJ, Maase, EL, Lin, HK, Madihally, SV, *Multilayer Composite Scaffolds with Mechanical Properties Similar to Small Intestine Submucosa.* J Biomed Mater Res A, 2009. 88(3): p. 634-643.

72. Pok, SW,Wallace, KN, Madihally, SV, *In Vitro Characterization of Polycaprolactone Matrices Generated in Aqueous Media.* Acta Biomater, 2009. 6(3): p. 1061-8.

73. Hutmacher, DW, Schantz, T, Zein, I, Ng, KW, Teoh, SH,c Tan, KC, *Mechanical Properties and Cell Cultural Response of Polycaprolactone Scaffolds Designed and Fabricated via Fused Deposition Modeling.* J Biomed Mater Res, 2001. 55(2): p. 203-16.

74. Lowry, KJ, Hamson, KR, Bear, L, Peng, YB, Calaluce, R, Evans, ML, Anglen, JO, Allen, WC, *Polycaprolactone/glass Bioabsorbable Implant in a Rabbit Humerus Fracture Model.* J Biomed Mater Res, 1997. 36(4): p. 536-41.

75. Kulkarni, RK, Moore, EG, Hegyeli, AF, *Biodegradable Poly(lactic acid) Polymers.* J Biomed Mater Res, 1971. 5(3): p. 536-41.

76. Dee, KC, Puleo, DA, Bizios, R, *An Introduction to Tissue-Biomaterial Interactions*. 2002: John Wiley & Sons.

77. Engelberg, I, Kohn, J, *Physico-mechanical Properties of Degradable Polymers Used in Medical Applications: A Comparitive Study.* Biomaterials, 1991. 12(3): p. 292-304.

78. Averous, L, Moroa, L, Doleb, P, Fringantc, C, *Properties of Thermoplastic Blends: Starch–Polycaprolactone.* Polymer, 2000. 41(11): p. 4157-4167.

79. Lee, JW, Kima, YH, Parkb, KD, Jeeb, KS, Shinc, JW, Hahna, SB, *Importance of Integrin β1-mediated Cell Adhesion on Biodegradable Polymers Under Serum Depletion in Mesenchymal Stem Cells and Chondrocytes.* Biomaterials, 2004. 25(10): p. 1901-9.

80. Massia, SP, Hubbell, J, *Covalently Attached GRGD on Polymer Surfaces Promotes Biospecific Adhesion of Mammalian Cells.* Ann N Y Acad Sci, 1990. 589(1): p. 261-70.

81. Zhang, H., Lin, CY, Hollister, SJ, *The Interaction Between Bone Marrow Stromal Cells and RGD-modified Three-dimensional Porous Polycaprolactone Scaffolds.* Biomaterials, 2009. 30(25): p. 4063-9.

82. Karakecili, A, Satriano, C, Gumusderelioglu, M, Marletta, G, *Relationship Between the Fibroblastic Behaviour and Surface Properties of RGD-immobilized PCL Membranes.* J Mater Sci Mater Med, 2007. 18(2): p. 317-9.

83. Lam, CXF, Mo, XM, Teoh, SH, Hutmacher, DW, *Scaffold Development Using 3D Printing with a Starch-based Polymer.* Materials Science and Engineering: C, 2002. 20(1-2): p. 49-56.

84. Liu, CZ, Xia, ZD, Han, ZW, Hulley, PA, Triffitt, JT, Czernuszka, JT, *Novel 3D Collagen Scaffolds Fabricated by Indirect Printing Technique for Tssue Engineering.* Journal of Biomedical Materials Research Part B Applied

Biomaterials 2008. 85 B(2): p.519-528.

85. Mao, JS, Zhao, L, Yin, YJ, Yao, KD, *Structure and Properties of Bilayer Chitosangelatin Scaffolds.* Biomaterials, 2003. 24(6): p. 1067-1074.

86. Harris, LD, Kim, BS, Mooney, DJ, *Open Pore Biodegradable Matrices Formed with Gas Foamin.* J Biomed Mater Res 1998. 42(3): p. 396-402.

87. Chun-Jen, L, Chin-Fu, C, Jui-Hsiang, C, Shu-Fung, C, Yu-Ju, L, Ken-Yuan, C, *Fabrication of Porous Biodegradable Polymer Scaffolds Using a Solvent Merging/Particulate Leaching Method. Journal of Biomedical Materials Research.* Journal of Biomedical Materials Research, 2002. 59(4): p. 676-681.

88. Wu, L, Jing, D, Ding, J, *A "Room-temperature" Injection Molding/Particulate Leaching Approach for Fabrication of Biodegradable Three-dimensional Porous Scaffolds.* Biomaterials, 2006. 27(2): p. 185-191.

89. Available from: http://en.wikipedia.org/wiki/Tissue_engineering.

90. Lawrence, BJ, Madihally, SV, *Cell Colonization in Degradable 3D Porous Matrices.* Cell Adhesion and Migration, 2008. 2(1): p. 1-8.

91. Rajnicek, A, Britland, S, McCaig, C, *Contact Guidance of CNS Neurites on Grooved Quartz: Influence of Groove Dimensions, Neuronal Age and Cell Type.* J Cell Sci, 1997. 110(23): p. 2905-2913.

92. Curtis, A, Wilkinson, C, *New Depths In Cell Behaviour: Reactions of Cells to Nanotopography.* Biochem Soc Symp, 1999. 65: p. 15-26.

93. Salem, AK, Stevens, R, Pearson, RG, Davies, MC, Tendler, SJ, Roberts, CJ, *Interactions of 3T3 Fibroblasts and Endothelial Cells with Defined Pore Features.* J Biomed Mater Res, 2002. 61(2): p. 212-217.

94. Zaleskas, JM, Kinner, B, Freyman, TM, Yannas IV, Gibson, LJ, Spector, M, *Growth Factor Regulation of Smooth Muscle Actin Expression and Contraction of Human Articular 58 Chondrocytes and Meniscal Cells in a Collagen-GAG Matrix.* Exp Cell Res, 2001. 270(1): p. 21-31.

95. Lee, CR, Grodzinsky, AJ, Spector, M, *The Effects of Cross-linking of Collagenglycosaminoglycan Scaffolds on Compressive Stiffness, Chondrocyte-Mediated Contraction, Proliferation and Biosynthesis.* Biomaterials, 2001. 22(23): p. 3145-3154.

96. Sieminski, AL, Hebbel, RP, Gooch, KJ, *The Relative Magnitudes of Endothelial Force Generation and Matrix Stiffness Modulate Capillary Morphogenesis In Vitro.* Exp Cell Res, 2004. 297(2): p. 574-584.

97. *Instron Tensile Testing*. Available from: http://www.instron.us/wa/applications/test_types/tension/default.aspx.

98. Scott, JH, *Scaffold Design and Manufacturing: From Concept to Clinic.* Advanced Materials, 2009. 21(32-33): p. 3330-3342.

99. Rajan, K, *Linear Elastic Properties of Trabecular Bone: A Cellular Solid Approach.* Journal of Materials Science Letters, 1985. 4(5): p. 609-611.

100. Harrison, NM, McDonnell, PF, O'Mahoney, DC, Kennedy, OD, O'Brien, FJ, McHugh, PE, *Heterogeneous linear elastic trabecular bone modelling using micro-CT attenuation data and experimentally measured heterogeneous tissue properties.* Journal of Biomechanics, 2008. 41(11): p. 2589-2596.

101. Mak, AF, *The Apparent Viscoelastic Behavior of Articular Cartilage The Contributions From the Intrinsic Matrix Viscoelasticity and Interstitial Fluid Flows.* Journal of Biomechanical Engineering, 1986. 108(2): p. 123-130.

102. Huang, C-Y, Mow, VC, Ateshian, GA, *The Role of Flow-Independent Viscoelasticity in the Biphasic Tensile and Compressive Responses of Articular Cartilage.* Journal of Biomechanical Engineering, 2001. 123(5): p. 410-417.

103. Wilson, W, v.Donkelaar, C, van Rietbergen, B, Ito, K, Huiskes, R, *Stresses in the local collagen network of articular cartilage: a poroviscoelastic fibril-reinforced finite element study.* Journal of Biomechanics, 2004. 37(3): p. 357-366.

104. Suh, J-K, Bai, S, *Finite Element Formulation of Biphasic Poroviscoelastic Model for Articular Cartilage.* Journal of Biomechanical Engineering, 1998. 120(2): p. 195-201.

105. García, JJ, Cortes, DH, *A nonlinear biphasic viscohyperelastic model for articular cartilage.* Journal of Biomechanics, 2006. 39(16): p. 2991-2998.

106. Thomas, GC, Asanbaeva, A, Vena, P, Sah, RL, Klisch, SM, *A Nonlinear Constituent Based Viscoelastic Model for Articular Cartilage and Analysis of Tissue Remodeling Due to Altered Glycosaminoglycan-Collagen Interactions.* Journal of Biomechanical Engineering, 2009. 131(10): p. 101002-101011.

107. Lieleg, O, Schmoller, KM, Claessens, MMAE, Bausch, AJ, *Cytoskeletal Polymer Networks: Viscoelastic Properties are Determined by the Microscopic Interaction Potential of Cross-links.* Biophysical Journal, 2009. 96(11): p. 4725-4732.

108. Sack, I, Beierbach, B, Wuerfel, J, Klatt, D, Hamhaber, U, Papazoglou, S, Peter Martus, JB, *The impact of aging and gender on brain viscoelasticity.* NeuroImage, 2009. 46(3): p. 652-657.

109. Farran, AJ, Teller, SS, Jha, AK, Jiao, T, Hule, RA, Clifton, RJ, Pochan, DP, Duncan, RL, Jia, X, *Effects of Matrix Composition, Microstructure, and Viscoelasticity on the Behaviors of Vocal Fold Fibroblasts Cultured in Three-Dimensional Hydrogel Networks.* Tissue Engineering Part A, 2009. 16(4): p. 1247-1261.

110. Frisoli, A, Borelli, LF, Stasi, C, Bellini, M, Bianchi, C, Ruffaldi, E, Di Pietro, G, *deformable soft tissues for computer assisted surgery.* Int J Med Robot, 2004. 1(1): p. 107-113.

111. Berkley, J, Turkiyyah, G, Berg, D, Ganter, M, Weghorst, S, *Real-time finite element modeling for surgery simulation: an application to virtual suturing.* IEEE Trans Vis Comput Graph 2004. 10(3): p. 314-325.

112. Famaey, N, Sloten, JV, *Soft tissue modelling for applications in virtual surgery and surgical robotics.* Comput Methods Biomech Biomed Engin 2008. 11(4): p. 351-366.

113. Yang, X, Church, CC, *A simple viscoelastic model for soft tissues in the frequency range 6-20 MHz.* IEEE Trans Ultrason Ferroelectr Freq Control, 2006. 53(8): p. 1404-1411.

114. Hollister, SJ, *Biosolid Mechanics: Modeling and Applications*. Fitting Quasilinear Viscoelastic Constitutive Model Constants; Available from: http://www.engin.umich.edu/class/bme456/ch8fitqlvconstant/bme456qlvfitmodel.htm

115. Cao, S, Rhinehart, RR, *A Self-Tuning Filter.* Journal of Process Control, 1997. 7(2).

116. Padmanabhan, V, Rhinehart, RR, *A novel termination criterion for optimization.* American Control Conference, 2005. 2284: p. 2281-2286.

117. Rhinehart, RR, *Optimization Applications*.Fall 2010, Oklahoma State University :Stillwater.

118. Shrowti, NA, Vilankar, KP, Rhinehart, RR, *Type-II critical values for a steady-state identifier.* Journal of Process Control, 2010. 20(7): p. 885-890.

119. Mirani RD, Pratt, J, Iyer, P, Madihally, SV, *The stress relaxation characteristics of composite matrices etched to produce nanoscale surface features.* Biomaterials, 2009. 30(5): p. 703-710.

120. Perie, DS, Maclean, JJ, Owen, JP, Iatridis, JC, *Correlating Material Properties with Tissue Composition in Enzymatically Digested Bovine Annulus Fibrous and Nucleus Pulposus Tissue* Annals of Biomedical Engineering, 2006.34(5): p 769-777.

VITA

Upasana Manimegalai Sridhar

Candidate for the Degree of

Master of Science

Thesis: PSEUDO-COMPONENT VISCOELASTIC MODELING OF SOFT TISSUES

Major Field: Chemical Engineering

Biographical:

Education:

- Completed the requirements for the Master of Science in Chemical Engineering at Oklahoma State University, Stillwater, Oklahoma, USA in December 2010.

- Completed the requirements for the Bachelor of Technology in Chemical Engineering at Sri Sivasubramaniya Nadar College of Engineering, Anna University, Tamil Nadu, India in May 2009.

Experience:

- Research Assistant to Dr. R. Russell Rhinehart, OSU, Aug 2009-Dec 2010.

- Teaching Assistant to Dr. Fahlenkamp for Graduate Process Modelling, OSU, Aug 2010-Dec 2010.

- Teaching Assistant to Dr. R. Russell Rhinehart for Graduate Optimization Applications, OSU, Aug 2009-Dec 2009.

Professional Memberships:

- Omega Chi Epsilon, OSU Chapter.

- International Society of Automation (ISA), OSU Chapter.

- American Institute of Chemical Engineers (AIChE), OSU Chapter.

- Indian Institute of Chemical Engineers (IIChE), SSN Student Chapter.

Name: Upasana Manimegalai Sridhar Date of Degree: December, 2010

Institution: Oklahoma State University Location: Stillwater, Oklahoma

Title of Study: PSEUDO-COMPONENT VISCOELASTIC MODELING OF SOFT TISSUES.

Pages in Study: 87 Candidate for the Degree of Master of Science

Major Field: Chemical Engineering

Scope and Method of Study:

Understanding the response of human tissues to externally imposed stress and strain is critical to improving quality of life. This work explored regression approaches and modeling that aid discovery and describe mechanisms of soft tissue structures.

The scope of the study is to develop a non-linear, multi-component, viscoelastic model using pseudo-component approach and to optimize the model parameters to best match the time-dependent experimental stress-strain data. This study also does qualitative testing to test the appropriateness and utility of the model. The models are developed using nonlinear optimization technique in MS Excel/ VBA for convenient access for others.

Findings and Conclusions:

Six composite models were developed using various combinations of viscoelastic components namely hyper-elastic spring, spring-and-dashpot, reform and retain component. Various optimization techniques such as RLM2, Cyclic and Leapfrogging were tested using the experimental stress time data and it was found that Leapfrogging was the most efficient and robust optimizer. 8 parameter models showed sufficiency in the number of parameters by best modeling PLGA, PCL and SIS data. The appropriateness of the models was studied by testing the models on literature data and also testing the models by generating cyclic stress-strain data. The models proved to be appropriate by returning expected results for the tests. The six composite models are made available for others along with the nonlinear optimization techniques as MS Excel/ VBA code.

ADVISER'S APPROVAL: Dr. R. Russell Rhinehart